Carpathian Journal of Earth and Environmental Sciences February 2023, Vol. 18, No. 1, p. 149 – 169; DOI:10.26471/cjees/2023/018/248

INTEGRATING LIDAR DATA, 2D HEC-RAS MODELING AND REMOTE SENSING TO DEVELOP FLOOD HAZARD MAPS DOWNSTREAM OF A LARGE RESERVOIR IN THE INNER EASTERN CARPATHIANS

Dan Lucian CIURTE[1,2], Alin MIHU-PINTILIE[3*], Andrei URZICĂ[2,4], & Adrian GROZAVU[2]

[1]Romanian Waters National Administration, Someş-Tisa Water Basin Administration, Maramureş Water Management System, St. Hortensiei 2A, 430294, Baia Mare, Romania, dan.ciurte@sgamm.dast.rowater.ro
[2]Faculty of Geography and Geology, Department of Geography, "Alexandru Ioan Cuza" University of Iaşi, Bd. Carol I 20A, 700505 Iaşi, Romania, dan.ciurte@sgamm.dast.rowater.ro, urzi-ca.andrei@student.uaic.ro, grozavu@uaic.ro
*[3]Institute for Interdisciplinary Research, Science Research Department, "Alexandru Ioan Cuza" University of Iaşi (UAIC), St. Lascăr Catargi 54, 700107 Iaşi, România, *Corresponding author: mihu.pintilie.alin@gmail.com, alin.mihu.pintilie@mail.uaic.ro*
[4]Research Center with Integrated Techniques for Atmospheric Aerosol Investigation in Romania, RECENT AIR, Laboratory of Interdisciplinary Research of Mountain Environment, Ion Gugiuman, Rarău Station for Research and Students Fellowships, 725100 Câmpulung-Moldovenesc, Suceava, România, urzica.andrei@student.uaic.ro

Abstract: The use of 1D, 2D, and 1D/2D modelling techniques to identify flood prone areas is a critical component of any flood hazard management project (e.g., APDF – action plan for dam failure) in the proximity of big dams and reservoirs. In this work, we manage to computed flood hazard models using 2D HEC-RAS module based on Digital Elevation Models (DEM's) derived from Light Detection and Ranging (LiDAR) data and pre- and post-processed using Geographic Information Systems (GIS)-based software (e.g., ArcGIS, HEC-RAS). Therefore, to produce urban flood hazard (FH) maps downstream of the Strâmtori-Firiza reservoir (S-Fr) in NW Romania, a multi-scenario approach based on LiDAR-derived DEM integration, 2D hydraulic modeling, and remote sensing (RS) data validation is provided. In this context, to assess the flood control capacity (FCC) of the S-Fr hydro-technical system, three flood tests based on S-Fr flow rate with 5% (167 m^3/s), 1% (270 m^3/s) and 0.1% (447 m^3/s) return periods were performed. The flood impact within the urban area of Baia Mare located downstream of S-Fr was achieved for each flood scenarios using four spatial data derived from the RAS Mapper module: flood extent (FE), flood depth (FD), flood velocity (FV) and flood hazard (FH). The results indicate that a large area of Baia Mare city can be affected by a potential flood caused by a dam failure and also contribute to the APDF update of S-Fr dam.

Keywords: 2D hydraulic modeling, LiDAR-derived DEM, complex hydro-technical works, urban flood hazard maps, flood vulnerability assessment, Strâmtori-Firiza reservoir, Inner Eastern Carpathians

1. INTRODUCTION

Over the last decade, extreme weather has reached catastrophic levels, especially in natural disasters manifestations (Albano et al., 2020; Alfieri et al., 2014; Clarke et al., 2022). Accordingly, the flood events have changed in frequency, magnitude, and their behavior (Blöschl et al., 2017; Hall et al., 2015; Rahmstorf & Coumou, 2011; Schneider et al., 2012). In this regard, the intensification of the hydrological regime due to the climatic changes conditions has made an unprecedented effect on the scale (Do et al., 2020; Mangini et al., 2018), spatial extent (Kundzewicz et al., 2013; 2018), duration (Serinaldi et al., 2018) and frequency (Najibi & Devineni, 2018) of flood events (Cîmpianu & Mihu-Pintilie, 2018). Therefore, in many studies dedicated to the related climate-natural disasters field indicates the fact that the occurrence and frequency of floods around the world have significantly increased under the drastic changes in climatic conditions (Alfieri

et al., 2015; Hirabayashi et al., 2013; Tabari, 2020; Thober et al., 2018). Additionally, according to the Emergency Events Database (EM-DAT) (Hoeppe, 2016), for the last half century, climate hazards have increased with 300% (Cîmpianu & Mihu-Pintilie, 2018), among them, flooding is the most common and damaging natural hazard on Earth after storms and earthquakes (Banholzer et al., 2014; Gigović et al., 2017; Wallemacq et al., 2015; Wilby & Keenan, 2012). Likewise, the increase of flood events has two main causes: (i) the direct implications of the climate change phenomenon and (ii) some negative socio-economic aspects like: changing floodplain functionalities induced by the land use practices (Cammerer et al., 2013; Rahman et al., 2021), urban development in flood risk areas (Feng et al., 2021; Huang et al., 2017), the increase of socio-economic activities (Dobrovičová et al., 2015) in flood-prone areas, accidents caused by dam failures, mismanagement and maintenance errors regarding the water storage, maintenance errors, strategic dam destruction or terrorism (Mihu-Pintilie, 2018) and, in some cases, by the inefficient planning policies in terms of flood risk reduction (Mustafa et al., 2018). Therefore, the consequences of human activity are most evident in urban area where the anthropogenic intervention on watercourses has profoundly modified the natural functionality of floodplains (Wheater & Evans, 2009). However, according to Vojtek & Vojteková (2016), under the pressure of modern society the population has exposed voluntarily to the flood hazard (FH).

Like in the case of many other European Union (EU) member states (Bubeck et al., 2017; Gralepois et al., 2016; Holguin et al., 2021), there is a lack in the flood mitigation strategy along the main watercourses in Romania (Cîmpianu et al., 2021; Romanescu et al., 2018, 2020; Stoleriu et al., 2020). This statement is supported by the large number of flood events that have occurred as a consequence of urban sprawl in high flood risk areas (Albano et al., 2020; Romanescu et al., 2017). Overall, this predicament results from the fact that most of Romania's current flood defense infrastructure and hydro-technical works were built between 1960 and 1970 in the communist period, with very few progresses made in the years that followed. In parallel, the urban territory development inside of the floodplains and river regularization efforts, along with increased deforestation in the Carpathian Mountains, have significantly altered the river discharge and flood regime (Arseni et al., 2020; Costache et al., 2021; Dumitriu, 2020; Popa et al., 2019).

The Firiza River (study area) has one of the most modified watercourses in the Someș river basin (NW Romania) (Sabău et al., 2022; Șerban et al., 2020). The hydro-technical works (most of them located in the lower sector of the Firiza valley) like Strâmtori-Firiza reservoir (S-Fr), as well as secondary dams, collector channels, transfer flows, protection works, and banks, have been constructed in order to reduce the risk of flooding and to build hydroelectric power plants (Ciurte et al., 2019). However, even if no significant flood events have occurred recently along the Firiza River, due to the recent modification in rainfall and flow regimes induced by climate change, human intervention on land cover and land use and, finally, by the increasing of sedimentation in the S-Fr, this situation can change at any time. Therefore, all these factors prove that Firiza River is really challenging in order to apply new FH assessment methodologies. However, since 2007, when Romania joined the EU, a first step in this direction has been taken and several FH and risk maps have been made under the Flood Directive 2007/60/EC of the European Council (EC) (Priest et al., 2016; Romanescu et al., 2020) by the employers of Romanian Waters National Administration (RWNA, 2022), including here also the Firiza watershed.

In addition to EC regulations described in the Floods Directive, the Ordinance no. 1422/192 from 16.05.2012 of the Ministry of Waters and Forests (RMWF) in Romania, each national water administration which own at least one reservoir with ≥ 10 m dam height and a storage capacity > 10 million m^3 have the obligation to provide an Action Plans for Dam Failure (APDF) (RGIES, 2022) hypothetical dam failure and analyze the potential material damage and human casualties (Urzică et al., 2021). In Romania, from more than 1,000 registered dams (250 big dams) only few of them have an APDF. In this case is also the S-Fr in the middle sector of the Firiza watershed (10 km north of Baia Mare) which has been operating since 1964. As in the case of other dams in Romania constructed during the communist period, the S-Fr reservoir has not yet an actualized APDF according to the national requirements concerning the flood risk reductions (RGIES, 2022). Therefore, based on the adopted methodology which involves 2D hydraulic modeling combining with remote sensing (RS) techniques and geographic in-formation systems (GIS) software, we plan to actualize the APDF for S-Fr and also to improve the existent official FH maps in the study site, respectively the lower Firiza Valley.

In this regard, in order to describe the methodology used in this approach which is relatively new in common FH assessment practices, it is important to be aware of the new tools and their capabilities regarding FH assessment (Samanta et al., 2018). Therefore, in many studies where 2D hydraulic modeling was performed for flood assessment purpose, accurate field-observed data at gauging station (e.g., flow rates, amount of precipitation) are requested but we need to pay a close attention to their accuracy and in

some cases, the flow data data are not available (Balica & Wright, 2009; Teng et al., 2017). Earth Observation (EO) products (e.g., aerial and satellite images) and GIS tools are also frequently used as secondary method to determine the flood extent (FE) in affected areas (Armenakis et al., 2017; Muthusamy et al., 2017; Pradhan et al., 2014; Wan et al., 2019). However, even if the RS technique offers accurate information related to hazard manifestation, this method it can be applied only for flood events that have already occurred (Quiroga et al., 2016).

In this framework we aim to develop a complex methodology in order to assess the FH under real (average flow rates) and mathematical (flow rates with different return period) hydrological data by combining LiDAR-derived digital elevation models (DEM), 2D HEC-RAS modeling and RS techniques. Therefore, we provided for the study site (Figure 1) the first accurate FH maps developed based on computed discharge for S-Fr and adapted to local environmental settings by using the DEM derived from LiDAR data. This new methodological approach represents the novelty of the work being in contrast with others studies where FH maps are provided based on hydrological data calibrated at river basin scale. Therefore, three 2D HEC-RAS scenarios with 5% (20-year), 1% (100-year) and 0.1% (1000-year) return periods were generated in order to test the impact of the S-Fr on flood mitigation on Firiza Valley. All scenarios were based on average discharge and calculated discharge at spillway gate of S-Fr and correlated with the official operating regulations of S-Fr dam. The results showed that a large area of Baia Mare City (Inner Eastern Carpathians, NW Romania) can be affected by a potential flood caused by a dam failure and also contribute to the APDF update of S-Fr dam and contribute to the APDF update of S-Fr.

Taking into account the above, in next sections the data used, and the techniques developed are presented and further implications of the study are discussed.

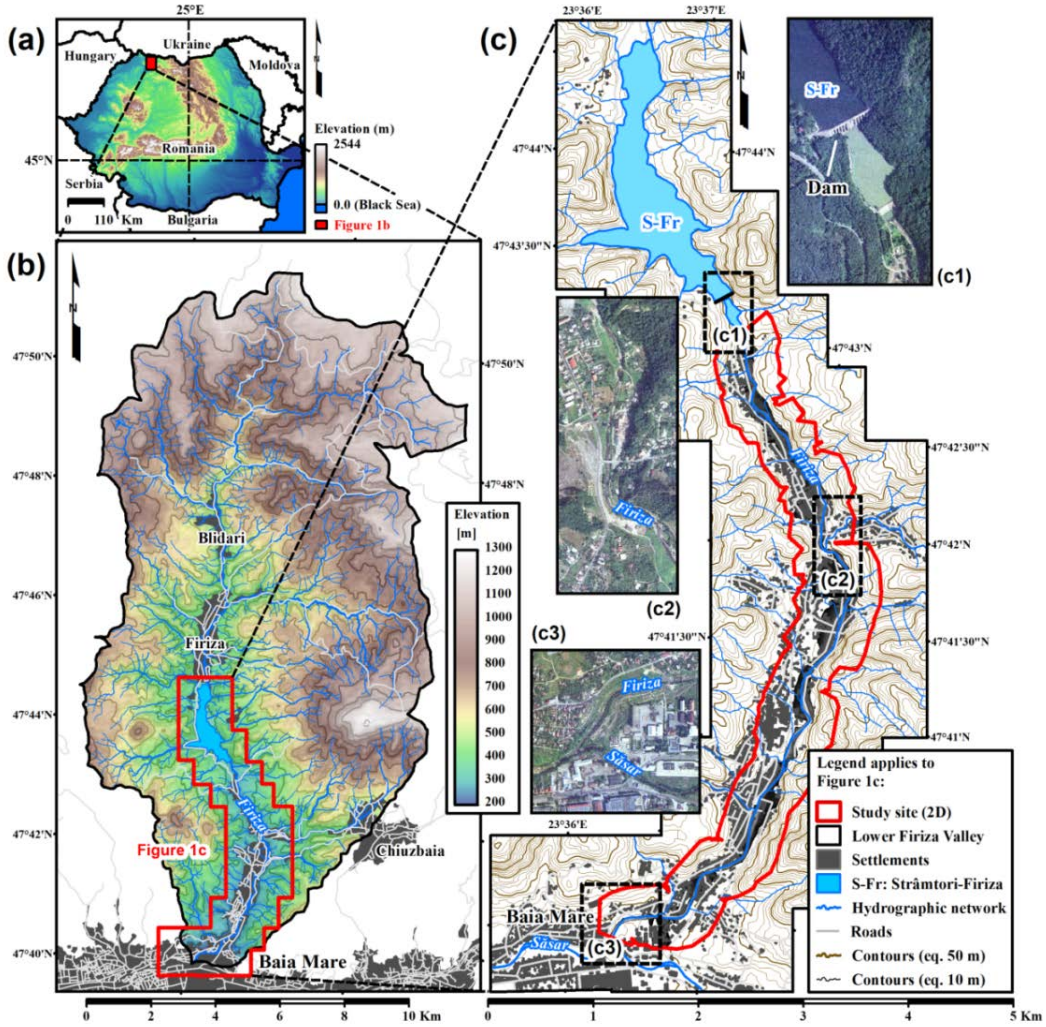

Figure 1. (a) Location in NW Romania of the **(b)** Firiza watershed; **(c)** The lower Firiza Valley sector and the study site used for 2D HEC-RAS modeling downstream of the Strâmtori-Firiza reservoir (S-Fr). In rectangles the **(c1)** S-Fr dam, **(c2)** Firiza watercourse and **(c3)** Firiza and Săsar rivers confluence on the Baia Mare territory are highlighted.

2. STUDY AREA

2.1. 2D Site: Lower Firiza Valley

The study area located in NW Romania (Figure 1a) overlaps with the lower sector of Firiza watershed (168.19 km^2) (Figure 1b) (Ciurte et al., 2019; Sabău et al., 2022; Şerban et al., 2020). With a 28 km length of main watercourse, the Firiza river is the most important affluent that flows into Săsar river (left tributary of Tisa River) (Şerban et al., 2020). The lowest elevation point is found at the confluence of Firiza and Săsar rivers (265 m) and the highest point is located in the eastern part of the Firiza watershed (Igniș Peak – 1,306.6 m a.s.l.). The lithology is characteristic of the upper Holocene deposits (e.g., alluvial deposits) accumulated over a complex segment of the Neogene and Quaternary volcanic chain of the Inner Eastern Carpathians (Lexa et al., 2017). The weather pattern control 60% to 70% of the flow rate, often overtaken in periods with heavy rains. The air temperature is ranges between 6.0°C (Igniș Peak station) and 9.7°C (Baia Mare station) between 1990 and 2021. The annual precipitation amount for the same period of time varies between 976 mm/year and 1500 mm/year, with peak values occurring in the north and east sectors of Firiza watershed (Sabău et al., 2022). The groundwater contributes with 40% of the annual flow rate. The multi-annual discharge at S-Fr inflow gauging station was 4.2 m^3/s, with a minimum flow rate of 1.8 m^3/s and a maximum flow rate of 7.3m^3/s, all values calculated for a period between 1990 and 2021 (Ciurte et al., 2019).

The study site used for 2D hydraulic modeling and urban FH assessment covers 4.34 km^2 in the northern extension of Baia Mare City (lower Firiza Valley) (Figure 1c). According to the last census, the town has a population of 137.976 inhabitants (17th largest city in Romania); in the study site, we estimate a number of people between 10,000 and 15,000 inhabitants (Ciurte et al., 2019. The considered Firiza River sector has 7.49km length be-tween S-Fr dam (367.5m) and common floodplain with Săsar River (265m). The maximum width of the study site does not exceed 1 km (max. width – 980 m in the lower sector of study site) and the main morphological aspects are characteristic for mountains valleys developed in the Inner Eastern Carpathians region. From 2D streamflow modeling perspective an accurate predictive flood model is difficult to achieve through classical methods due to the complex hydro-technical works which equip the lower Firiza Valley. However, according to SMIS-CSNR (2022), the fact that Baia Mare City is one of the most vulnerable cities in Romania, is not highlighted by the FH maps. Therefore, the urban area of Baia Mare has grown steadily over the past 20 years, and new constructions in the Firiza floodplain up to the vicinity of the S-Fr (Figure 2) are at risk of being flooded (Ciurte et al., 2019; Sabău et al., 2022; Şerban et al., 2020).

2.2. Strâmtori-Firiza reservoir and dam

The Strâmtori-Firiza reservoir (S-Fr) is the main reservoir of the Baia Mare hydro-technical system, being located 10 km upstream on the Firiza River (Ciurte et al., 2019) (Figure 2a). Based on the National Classification of Reservoirs and Lakes, the S-Fr is classified as special importance (category A) and in the first class of importance (SMIS-CSNR, 2022) due to the fact that is the single dam in the region located in the proximity of a big city (Baia Mare). The S-Fr dam, a concrete mushroom-head buttress dam with 51.5 m high and 260 m length, was designed and completed between 1960 and 1964 (Figure 2b). The entire S-Fr hydro-technical system was built-up to ensuring the water supply for drinking and industrial water in the Baia Mare mining micro-region and for production of electricity using hydro-power plants (Lexa et al., 2017). Regarding the flood control capacity (FCC), although the S-Fr has a normal water level (NWL) of 15.67 million m^3 (equivalent to flood control level with 5% return periods) the parameters determined by the operating conditions restrict the attenuation volume to only for 0.849 million m^3. Therefore, the flood defense downstream of S-Fr (study site) is achieved under high water conditions by using the spillways that can release a maximum discharge of 270 m^3/s (equivalent to flood control level with 1% return periods), operations limited also by the 110 m^3/s transport capacity of the lower riverbed sector of Firiza Valley. However, being the oldest dam in the region, the rehabilitation and conditional exploitation of S-Fr are necessary. More detailed related to water volume and surface ratio at different storage capacity and the flood control level for 1% and return period for S-Fr are highlighted in Figure 2b (Ciurte et al., 2019).

3. MATERIALS AND METHODS

The workflow chart or workflow diagram is summarized in Figure 3, with LiDAR processing, bathymetric model processing, hydrological data correlation and construction data collection, and the key steps for 2D HEC-RAS modeling. The FCC of the Firiza Valley in case of Q_{max} (m^3/s) flow rates calculated for 5%, 1% and 0.1% return periods has been computed using the raster results exported from RAS Mapper module (flood extent – FE, flood depth – FD, flood velocity – FV and flood hazard – FH) (AIDR, 2017), within urban area downstream of S-Fr (study site in Figure 1c).

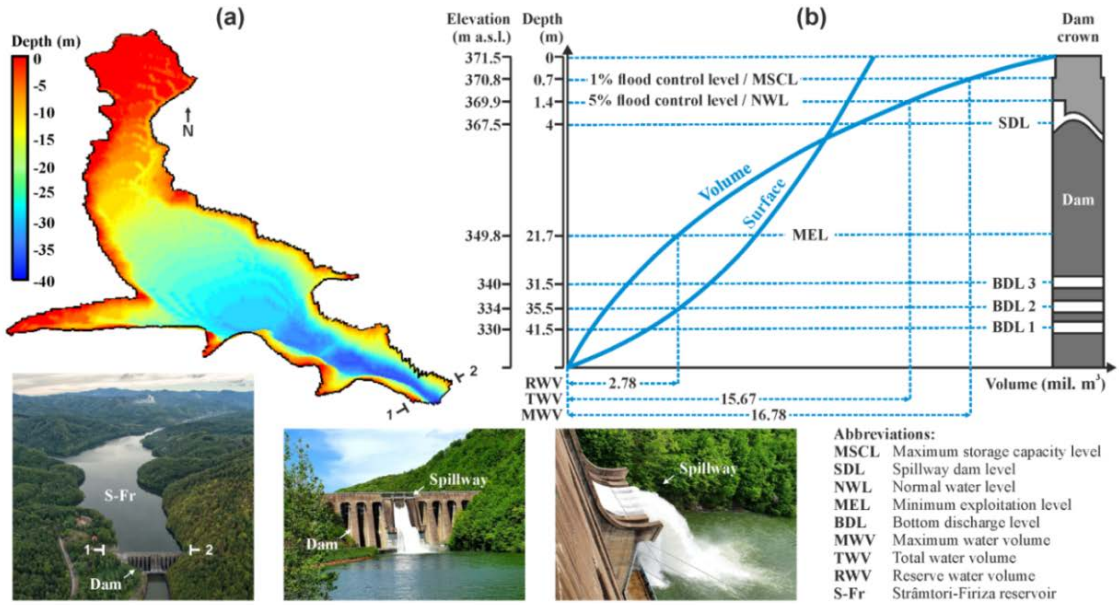

Figure 2. **(a)** 3D bathymetric model of Strâmtori-Firiza water accumulation (S-Fr) and **(b)** a sketch of S-Fr dam with characterization of water volume and surface ratio at different storage capacity and the flood control level for 1% and 5% return period. In photos the S-Fr dam and spillway gate are highlighted.

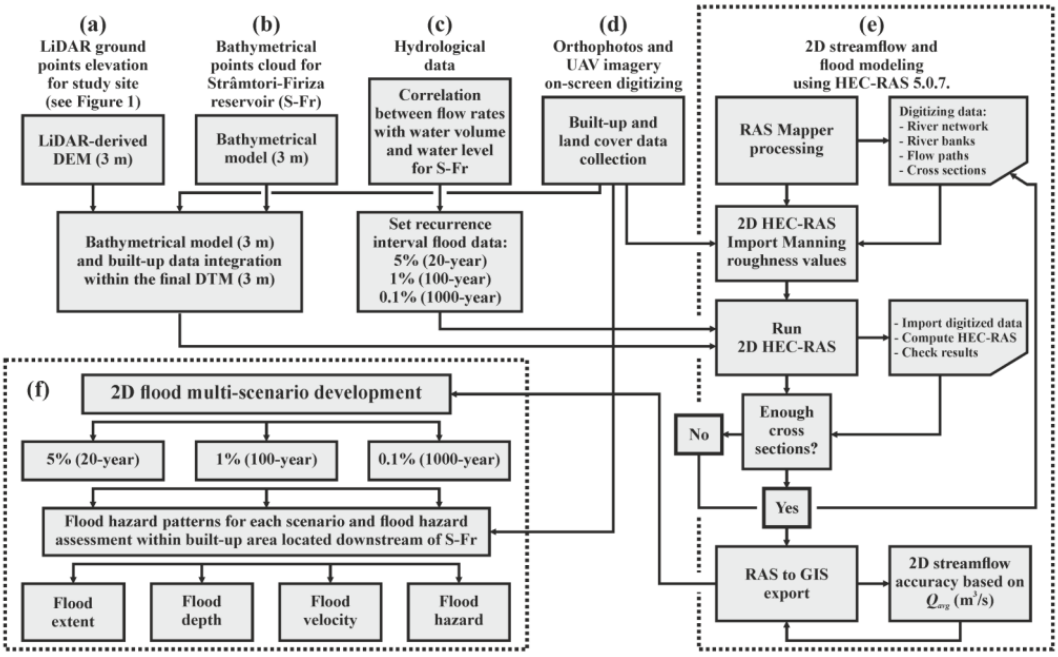

Figure 3. Flowchart of the 2D flood modeling process, where: **(a)** LiDAR ground points elevation and **(b)** bathymetrical data has been used to improve the final DEM and **(c)** hydrological data to correlate the S-Fr outflow rates; **(d)** the land cover data and the constructions integration in final DTM; **(e)** detailed steps regarding the 2D HEC-RAS flood modeling, flow accuracy assessment based on Q_{avg} (m^3/s) flow extent and RAS to GIS export; **(f)** generate the flood pattern (FE, FD, FV) and FH assessment using the AIDR methodology.

3.1. Data acquisition

3.1.1. Development of LiDAR-derived DEM

The Strâmtori-Firiza reservoir (S-Fr) is the main During 2007/60/ EC Directive and SMIS-CSNR No.28988 project: The plan for the prevention, protection and mitigation of the effects of floods in the Someș-Tisa River Basin (S-TRB) in 2015 (SMIS-CSNR, 2022), the entire territory of the study site was scanned with LiDAR technology (Figure 3a). Therefore, by using ArcGIS software we manage to appended in a new raster dataset with a spatial resolution of 3 m/pixel all available DEM's (>100 raster files). Next step was to integrate within the final DEM all the anthropic constructions (post-2018) like: houses, attachment buildings, administrative buildings, and industrial buildings, so one (Arief et al., 2018; Kim, 2016; Yu et al., 2010).

The built-up data was obtained by vectorization process in ArcGIS software using two main background data sources: orthopothos and Unmanned Aerial Vehicle (UAV) imagery collected in different areas of study site. Furthermore, in order to rasterize the construction data and join to the final DEM, a 5 m elevation for each building in the study area was assigned (Figure 3a).

3.1.2. S-Fr bathymetric model

To generate the HEC-RAS models we merged the S-Fr bathymetric data (Figure 2a) within the LiDAR-derived DEM obtained in the previous step (Figure 3b). The bathymetry of the S-Fr was obtained by the Maramureș Water Management System, Someș-Tisa Water Basin Administration (MWMS – S-TWBA) (SMIS-CSNR, 2022). The bathymetric measurements were made in 2011 and > 80,000 depth points were obtained. By processing the depth points (Mihu-Pintilie et al., 2014), a final raster with a spatial resolution of 3 m/pixel was generated (Ciurte et al., 2019) and GIS-based integrated in the final DEM used for 2D modeling. However, in order to join the bathymetry of the S-Fr with LiDAR-derived DEM, a new Raster Dataset was created and the LiDAR-derived DEM was joined with the S-Fr bathymetric model (Figure 3b) (Urzică et al., 2021).

3.1.3. S-Fr outflow data

The discharge data used for 5% (20-year), 1% (100-year) and 0.1% (1000-year) return periods computation (Figure 3c) consist in inflow (Figure 4a), outflow (Figure 4b) and water balance (Figure 4c) discharge Q(m^3/s) data of Strâmtori-Firiza reservoir (S-Fr) between 1990 and 2021. All data was obtained from the employers of MWMS – S-TWBA.

According to the Official Operating Rules (OOR) of Strâmtori-Firiza reservoir (S-Fr) which was classified after the height of the dam (51.5 m) and storage capacity volume (17.39 million m^3), in the first importance category in Romania, the flow rates calculated for calibration the 2D HEC-RAS modeling are: 167 m^3/s for 5% (20-year) return period, 270 m^3/s for 100-year return period and 447 m^3/s for 1000-year return period (RWNA, 2022). In Table 1 are indicate the further details on the water surface area (m) and volume (million m^3) of the S-Fr at various Q_{max} (m^3/s) flow rates.

Table 1. The water volume (million m^3) and surface characteristics (m) in the Strâmtori-Firiza reservoir at different Q_{max} (m^3/s) flow rates calculated for 20-year, 100-year and 1000-year return periods

Return period	Water volume (Million m^3)	Water surface elevation (m)	Q_{max} (m^3/s)
20-year	15.67	369.90	167
100-year	16.62	370.80	270
1000-year	17.39	371.50	447

3.1.4. Land cover data

Using on-screen digitizing techniques, we obtained the land use data from two main background data sources: orthophotos (2015 and 2018 editions) and Unmanned Aerial Vehicle (UAV) imagery collected in different areas of study site (Figure 3d). Therefore, there were obtained 17 land cover classes according to the Corine Land Cover (CLC) classification (Feranec et al., 2010; Kucsicsa et al., 2019; Rusu et al., 2020): discontinuous dense urban fabric (Code 112.1: 50% - 80%); discontinuous medium density urban fabric (Code 112.2: 30% - 50%); discontinuous low density urban fabric (Code 112.3: 10% - 30%); discontinuous very low density urban fabric (Code 112.4: <10%); isolated structures (Code 133); industrial, commercial, public, military and private units (Code 121); land without current use

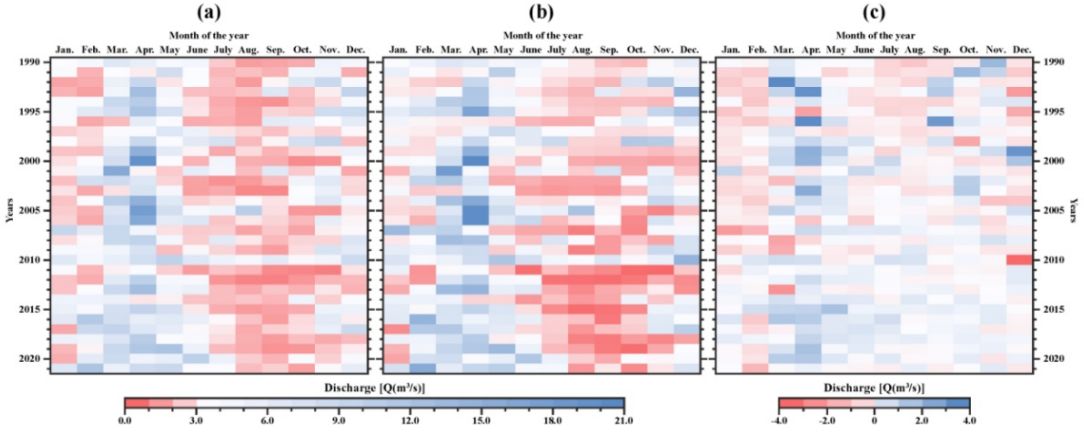

Figure 4. Raster hydrographs shows **(a)** inflow (iS-Fr) and **(b)** outflow (oS-Fr) average monthly discharge Q (m^3/s) of Strâmtori-Firiza reservoir (S-Fr) between 1990 and 2021. In figure **(c)** the water balance (iS-Fr / oS-Fr) of S-Fr are indicated, where negative values represent iS-Fr > oS-Fr and positive values represents iS-Fr < oS-Fr.

(Code 134); sports and leisure facilities (Code 142); arable land (annual crops) (Code 211); pastures (Code 231); forests (Code 313); water (Code 511); roads and associated roads land, railways and railways and associated land (Code 122). After the final validation of land use data in the study site were digitized more than 5,000 polygons features (minimum mapping unit of 30 m^2).

3.2. Hydraulic modelling

3.2.1. 2D HEC-RAS modelling

The HEC-RAS is open-source software released in 1995 by U.S. Army Corps of Engineers (USAGE) with the capability in FH modeling (Balica & Wright, 2009; Brunner, 2016a, 2016b; Samanta et al., 2018; Teng et al., 2017). In this study, all flood scenarios were computed using the 5.0.7 version of the HEC-RAS.

Overall, the FH modeling based on HEC-RAS software requires accurate data regarding the terrain data (e.g., DEM derived roughness coefficient) and flow data (e.g., river discharge). HEC-RAS software is able to simulate FH using three different methods: one-dimensional unsteady flow model (Bush et al., 2022), two-dimensional unsteady flow model and hybrid 1D–2D modeling (Brunner, 2020; Jonoski et al., 2019; Mitsopoulos et al., 2022; Samarasinghe et al., 2022).

Considering that downstream of the S-Fr is a highly populated area and we obtained accurate data for the site area (e.g., LiDAR-derived DEM, bathymetric model, hydrological data, roughness coefficient for all land use categories), the 2D modeling is the best method in order to test the FE in the lower sector of Firiza Valley. Furthermore, for a 2D accuracy models we choose to represent the urban areas by integrated the buildings in the final LiDAR-derived DEM (see sub-section LiDAR Data). One of the advantages of the 2D hydraulic models is that we can capture the changes (the increases and decreases) of the water depth or water velocity for each cell. Considering that HEC-RAS software is able to generate unsteady flow routing using two different equations: (1) full Saint Venant (also called full momentum equation) and (2) & (3) diffusion wave equation (Brunner, 2016a, 2016b; Mehedi et al., 2022; Yazdan et al., 2022), we created 2D models with Equation (1), Equation (2) and Equation (3). We use the diffusion wave equation based on the best similarity results (Cîmpianu & Mihu-Pintilie, 2018). However, this equation is recommended to be used in order to acquire a high stability of the models and a faster computational time.

In this framework, the storage area extents (study site) were imported in the RAS Mapper module and create the sub-grid model (mesh; Figure 5a) which represents a polygonal network where each cell has information about the underlying terrain. In 2D modelling each cell from the mesh is similar to a cross-section from the 1D hydraulic modeling. Therefore, the 2D flow area (Figure 5a) directly connected with S-Fr dam was created based on the FE which consists in > 67,000 cells with 64 m^2 each. In this way, we can capture as many LiDAR-derived terrain characteristics as possible.

The last step in RAS Mapper processing was to set the roughness coefficients specific to each land cover category from the study site. In this context, due to the fact that the study site a typical mountain floodplain area, the floodplain roughness of the land uses categories was assigned according to Gallegos et al., (2009) specifications (Figure 5b). After the geometries were created and the roughness coefficient was set, the first step in 2D streamflow modeling consists by setting the boundary conditions (BC). In this step we choose the start point and the end point of the FE within the flow area.

Therefore, for the upstream boundary condition (U-BC) which represent the start point of the flood wave we used the flow hydrographs and for the downstream boundary condition (D-BC) which represent the end point of the flood wave we used the normal depth boundary conditions (BC) which means

$$\frac{\partial \zeta}{\partial t} + \frac{\partial p}{\partial x} + \frac{\partial q}{\partial y} = 0 \quad (1)$$

$$\frac{\partial p}{\partial t} + \frac{\partial}{\partial x}\left(\frac{p^2}{h}\right) + \frac{\partial}{\partial y}\left(\frac{pq}{h}\right) = -\frac{n^2 p g\sqrt{p^2+q^2}}{h^2} - gh\frac{\partial \zeta}{\partial x} + pf + \frac{\partial}{\rho \partial x}(h\tau_{xx}) + \frac{\partial}{\rho \partial y}(h\tau_{xy}) \quad (2)$$

$$\frac{\partial q}{\partial t} + \frac{\partial}{\partial y}\left(\frac{q^2}{h}\right) + \frac{\partial}{\partial x}\left(\frac{pq}{h}\right) = -\frac{n^2 q g\sqrt{p^2+q^2}}{h^2} - gh\frac{\partial \zeta}{\partial y} + qf + \frac{\partial}{\rho \partial y}(h\tau_{yy}) + \frac{\partial}{\rho \partial x}(h\tau_{xy}) \quad (3)$$

Where: h – water depth (m); p – specific flow for x directions (m^2s^{-1}) and q – specific flow for y directions (m^2s^{-1}); ζ – surface elevation (m), g – gravitational acceleration (ms^{-2}); n – Manning's roughness coeff.; ρ – water density (kg m^{-3}), τ_{xx}, τ_{yy}, and τ_{xy} – effective shear stress components; f – Coriolis (s^{-1}). When the diffusive wave is selected the inertial terms of the momentum equations are neglected (Eq. (2) and Eq. (3)).

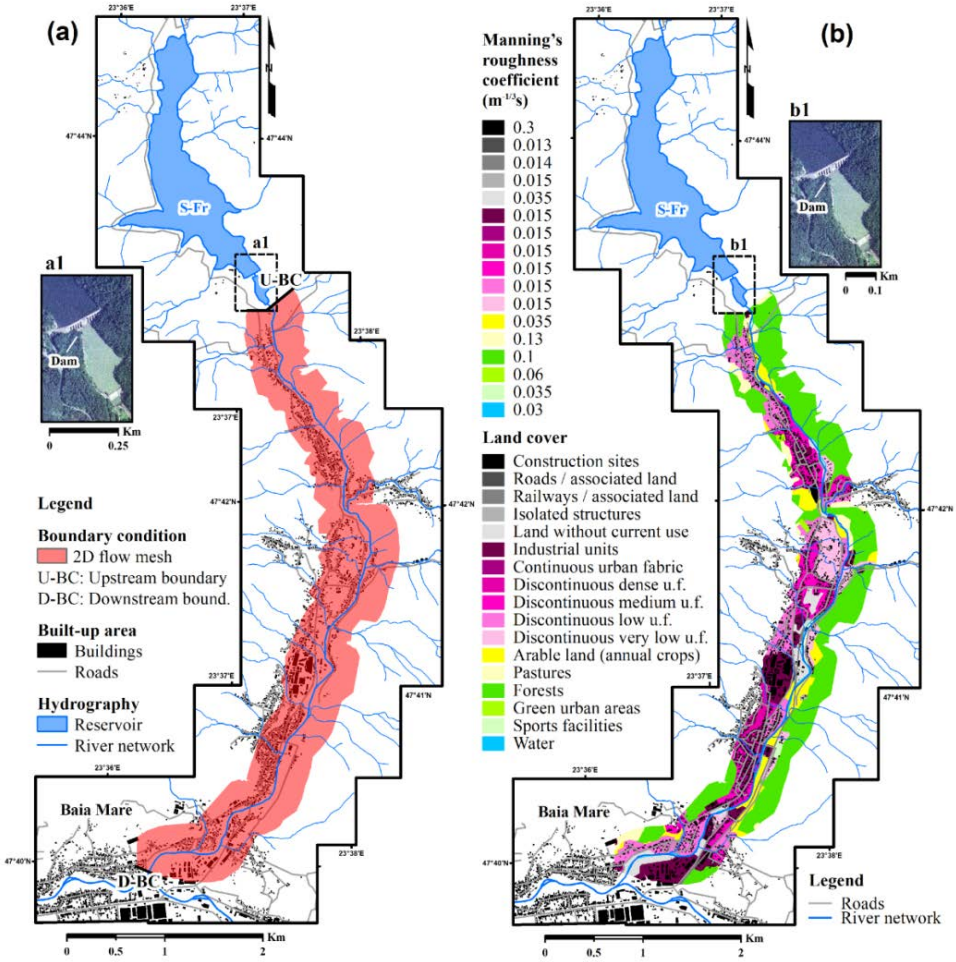

Figure 5. 2D hydrological model calibration downstream of the Strâmtori-Firiza reservoir (S-Fr): **(a)** Boundary condition along with 2D flow area and flow mesh on the study site; **(b)** Land use map within study site and Manning's Roughness coefficient n ($m^{-1/3}s$) value for each class.

the average of the riverbed slope. In our case study, three scenarios were simulated, and a hydrograph and the normal depths boundary conditions were applied to each flood model outcome. Each flow hydrograph was 24 h long with hourly recorded values. The U-BC where the hydrographs represent the start point of the flood wave is set at the spillway gate of S-Fr dam, and the D-BC is set at the limits of LiDAR-derived DEM, near to Firiza and Săsar confluence and an energy slope equivalent to 10^{-4} mm^{-1} was set (Figure 5a).

The estimation of the computational time is a crucial stage in 2D modeling projects. The stability of the 2D HEC-RAS hydraulic models might be impacted by incorrect calculation time. In more words, a big-time step can create the attenuation of the flood peak and a small-time step can lead to a very long computational period. For the proper computational time we used the Courant Condition (Equation (4)):

$$C = \frac{V_w \Delta T}{\Delta X} \leq 1; \quad \Delta T = \frac{\Delta x}{V_w}; \quad V_w = \frac{dQ}{dA} \qquad (4)$$

Where: C – Courant number; ΔT – time step (s); Δx – distance step (m) or avg. two-dimensional cell size; V_w – flood wave speed (m/s); dQ – flow change over a short time interval ($Q_2 - Q_1$); dA – cross section area change over a short time interval ($A_2 - A_1$). According to Equation (4) a time step of 10 seconds was used to run the model.

3.2.2. 2D HEC-RAS simulation accuracy

In order to run the 2D HEC-RAS flood modelling based on computed discharge (see Table 1), a flow test was performed to see the calibration accuracy of the hydrologic modelling project (e.g., boundary condition) and hydraulic stability of the used LiDAR-derived DEM (Ahmad et al., 2022; Awadallah et al., 2022).

Therefore, based on the daily average discharge values registered at outflow and a Sentinel-2 optical ground-projected image extracted from the study site showing the water extent in the same date the assessment of the flow accuracy was made.

The results indicate a similarity of 91% between the water extent generated by the 2D hydraulic computation for average discharge value and the water extent extracted from the Sentinel-2 optical image according to Romanescu et al., (2017) methodology. However, considering that in our study site the vegetation may cover the water surface in some sectors, and also, the low resolution of Sentinel-2 scene comparing with DEM resolution (Cîmpianu et al., 2021; Mihu-Pintilie et al., 2019), the test results are considered satisfactory. In this framework, we decided to run the 2D flood models by using all hydrological settings and data input in RAS Mapper processing.

3.2.3. Flood multi-scenario development

The flood scenarios with 5%, 1% and 0.1% return periods were computed using the hydrological measurements obtained from the Strâmtori-Firiza reservoir (S-Fr) official operating rules. For all three scenarios, upstream boundary conditions (U-BC) were created with a temporal precision of one hour during the water flow for a period of 24 hours (see Figure 5a). The average discharge scenario used for flood simulation accuracy in the previous section was carried out under the same conditions. Therefore, in case of first scenario (S1) with 5% (20-year) return periods take into consideration a discharge of 167 m^3/s, in case of second (S2) scenario with 1% return period a discharge of 270 m^3/s and in case of third scenario (S3), a discharge of 447 m^3/s with 0.1% return period (Table 1).

3.3. Flood impact assessment

Generally, there are many studies dedicate to the flood impact assessment in urbanized areas of which the most used classification methods are based on the FE (Cîmpianu et al., 2021; Mihu-Pintilie et al., 2019; Stoleriu et al., 2020). In this approach, we employed the FD·FV raster product from RAS Mapper to categorize the flood risk.

According to the technique developed by the employers of the Institute for Disaster Resilience from Australian (AIDR, 2017), we divided the flood danger severity into 6 classes:

- H1 (FD·FV ≤ 0.3 m^2/s)
- H2 (FD·FV range between > 0.3 m^2/s and ≤ 0.6 m^2/s)
- H3 (FD·FV range between >0.6 m^2/s and ≤ 1.2 m^2/s)
- H4 (FD·FV range between > 1.2 m^2/s and ≤ 2 m^2/s)
- H5 (FD·FV range between >2 m^2/s and ≤ 4 m^2/s)
- H6 (FD·FV > 4 m^2/s) (Table 2).

4. RESULTS

4.1. Flood pattern

To analyze the FE pattern, we used the Inundation Boundary generated by RAS Mapper module. To flood impact assessment, water depth and water velocity as raster files were computed. Therefore, HEC-RAS has the capability to export as vector and raster files each hydraulic scenario: S1 – 5% (20-year), S2 – 1% (100-year) and S3 – 0.1% (1000-year) return periods (Figure 3f).

4.1.1. Flood extent (FE)

The hypothetical flooding events downstream of the S-Fr according to the three hydraulic scenarios results can flood an area of 54.07 ha (from which 17.56 ha urban area) for the S1, 75.19 ha (from which 25.44 ha built-up area) for the S2, and 103.66 ha (from which 40.07 ha urban area) for the S3 (Figure 6). Based on the FE results for each scenario, we can conclude that the Firiza Valley (study site) response proved to be not effective in diminishing the FE. We support this statement by the fact that the magnitude of the floods increases exponentially from the scenario with the lowest return period (5%) to the worst one (0.1%). According to a thorough analysis of the built-up areas that could be impacted by floods, 380 buildings (15.68% of buildings) could be impacted by floods in the case of a S1, 609 buildings (25.15% of buildings) in case of S2, and 910 buildings (37.57% of the buildings) in the case of S3 (Table 3).

Table 2. FH classification developed by AIDR.

Hazard classes	* FD·FV (m^2/s)	FH description
H1	≤ 0.3	Generally safe vehicles, people and buildings
H2	≤ 0.6	Unsafe for small vehicles
H3	≤ 1.2	Unsafe for vehicles, children and the elderly
H4	≤ 2	Unsafe for vehicles and all category of inhabitants
H5	≤ 4	All the construction types vulnerable to structural damage and / or to failure
H6	> 4	All construction types considered vulnerable to failure.

* FD – flood depth; FV – flood velocity.

Table 3. The impact of each flood scenarios within urban area downstream of the S-Fr computed for each scenario with 5%, 1% and 0.1% return periods.

Land use category / code	Return periods		
	5%	1%	0.1%
Discontinuous urban fabric / 112.1 (ha)	0.01	0.41	0.96
Discontinuous urban fabric / 112.2 (ha)	3.01	4.49	7.13
Discontinuous urban fabric / 112.3 (ha)	2.26	3.69	7.04
Discontinuous urban fabric (ha) / 112.4`	7.99	9.99	13.03
Isolated structures / 133 (ha)	0.27	0.36	0.37
Industrial, commercial, public, military and private units / 121 (ha)	1.74	2.94	6.49
Land without current use / 134 (ha)	1.38	1.96	3.04
Sports and leisure facilities / 142 (ha)	0.83	1.11	1.24
Arable land (annual crops) / 211 (ha)	4.17	6.60	9.07
Pastures / 231 (ha)	1.20	1.65	2.61
Forests / 313 (ha)	28.43	37.30	45.28
Water / 511 (ha)	1.33	2.24	3.59
Roads (km)	3.87	6.08	9.19
Associated roads land (ha)	0.65	1.05	2.02
Railways and associated land (ha)	0.80	1.40	1.79
Total affected area (ha)	**57.94**	**81.27**	**112.9**
Buildings (no.)	380	609	910
Railways (km)	0.29	0.9	1.58

For the first FH scenario (5%, 20-year), the 54.07 ha is potentially affected of which 17.56 ha within urban area. The worst affected land use categories are the forest vegetation area (28.43 ha), discontinuous urban fabric (13.27 ha), arable land / annual crops (4.17 ha), industrial areas (1.74 ha), land without current use (1.38 ha), pastures (1.2 ha), water body / wetlands (1.33 ha), as well as 3.87 km of roads and 0.29 km of railways. The following land use categories are affected <1 ha: isolated structures, leisure facilities, associated roads land, railways and associated land. Referring to the inhabitants located downstream of the S-Fr who can be potentially affected by FE with 5% return period we estimate a number between 750 and 1,000 people.

In the second scenario (1%) an area of 75.19 ha are affected by FE of which 25.44 ha within urban area As in case with S1, also the most affected land use categories are the forest vegetation area (37.30 ha), discontinuous urban fabric (18.58 ha), arable land / annual crops (6.6 ha), industrial units (2.94 ha), land without current use (1.96 ha), water body or wetlands (2.24 ha), pastures (1.65 ha), sports and leisure facilities (1.11 ha), as well as 6.08 km of roads (associated roads land – 1.05 ha) and 0.9 km of railways (railways and associated land – 1.4 ha). Other land use category which has the potentially affected surface below 1 ha remain the isolated structures (0.36 ha). Referring to the Firiza Valley inhabitants, we estimate a number situated between 1250 and 1500 people who can be affected by FE with 1% return period.

In case of S3 (0.1%) 103.66 ha can potentially affected by FE of which 40.07 ha within urban area. The most affected land use categories within study site over 5 ha are the forest vegetation area (45.28 ha), discontinuous urban fabric (28.16 ha), arable land / annual crops (9.07 ha), industrial units (6.49 ha), as well as 9.19 km of roads (associated roads land – 2.02 ha) and 1.58 km of railways (railways and associated land – 1.79 ha). The rest of land use category totals over 10 hectares. Referring to the number of inhabitants located in the study site we estimate between 1500 and 2000 people which can be affected by FE with 0.1% return period.

4.1.2. Flood depth (FD)

The FD raster is the second parameter generated in the RAS Mapper module and used to develop urban FH maps downstream of the S-Fr. The FD was computed for each cell based on the LiDAR-derived DEM in the study site and the maximum FD value of the each cell from the beginning and to the end of the hydraulic simulation. Therefore, three raster files with FD corresponding to each scenario with 5% (20-year), 1% (100-year) and 0.1% (1000-year) return periods has been obtained and exported to GIS (Figure 3e,f).

The results obtained for 5% (20-year) return period scenario showed that the maximum FD value is 4.8 m and corresponds to the thalweg of the Firiza River. A percentage of 80% of the buildings (304 buildings) can be potentially damaged by a FD of <1.0 m, 18.95% (72 buildings) by a FD between 1.0 to 2.0 m and only 4 structures (1.05%) are potentially damaged by a flood wave with a depth between 2.0-3.0 m (Table 4).

For the second scenario with 1% (100-year) return period the maximum depth is 5.4 m and 74.9% of the constructions (456 buildings) are potentially damaged by a FD of <1 m, 18.55% (113 buildings) by a FD between 1.0 and 2.0 m, and 40 structures (6.6%) are potentially damaged by a flood wave depth between 2.0 and 3.0 m. The results regarding S1 and S2 are similar in therms of FD classes and flood impact (Table 4). In the case of the S3 (0.1%) the maximum value of the FD is 7.0 m and corresponds to the thalweg of the Firiza River (Figure 7). A percentage of 60.1% (547 buildings) of buildings could be impacted by floods that are less than 1.0 m deep, 26.5% (241 buildings) by floods that are between 1.0 and 2.0 m deep, 10.3% (94 buildings) by floods that are between 2.0 and 3.0 m deep, and 3.1% (28 buildings) by floods that are between 3.0 and 4.0 m deep (Table 4).

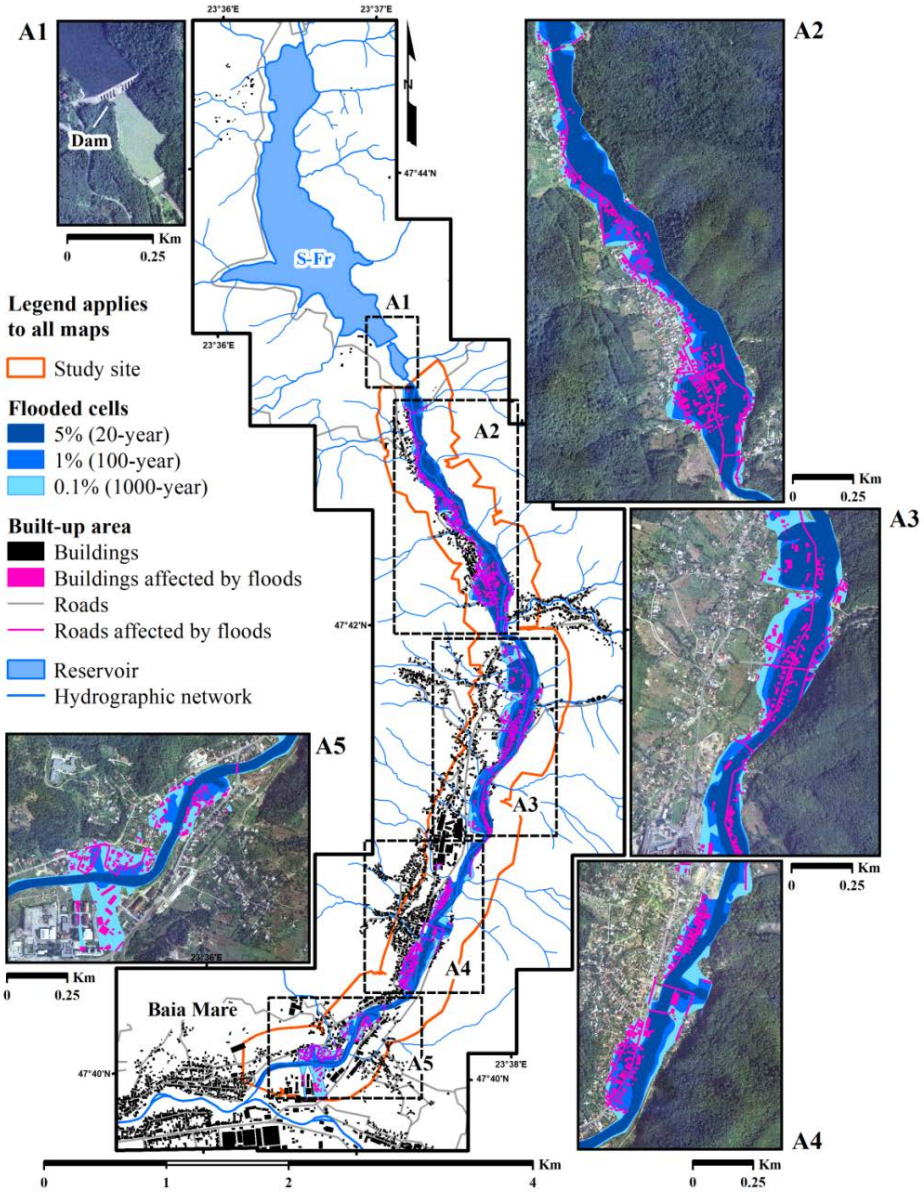

Figure 6. FE within urban area located computed for each scenario with 5%, 1% and 0.1% return periods (A1-A5: zoom into the study area).

Table 4. FD (m) and number of buildings potentially affected by the floods computed for each scenario with 5%, 1% and 0.1% return periods.

FD (m)	Return period		
	20-year	100-year	1000-year
<1	304	456	547
1-2	72	113	241
2-3	4	40	94
3-4	-	-	28

4.1.3. Flood velocity (FV)

The FV is the third raster product generated in the RAS Mapper module and used to develop urban FH maps downstream of the S-Fr. The FV values were generated similar with the FD raster and three raster files with FV corresponding to each scenario with 5%, 1% and 0.1% return periods (Figure 8). has been exported from RAS Mapper to ArcGIS (Figure 3e,f).

The FV values for each hydraulic scenario are greater than 5 m/s: 5.66 m/s for the 5% return period, 6.38 m/s for the 1% return period, and 10.44 m/s for the 1% return period (Table 5). The maximum values obtained for the FV can be attributed to the relief conditions (steep slopes) and land use categories (>40% urban area) in the Firiza Valley which induced a low roughness.

Based on the 5% (20-year) return period scenario a maximum value of the 13.61 m^2/s was obtained along the Firiza floodplain downstream of the S-Fr. In the study site, 34.02% of the total potentially affected areas are classified as H1 hazard

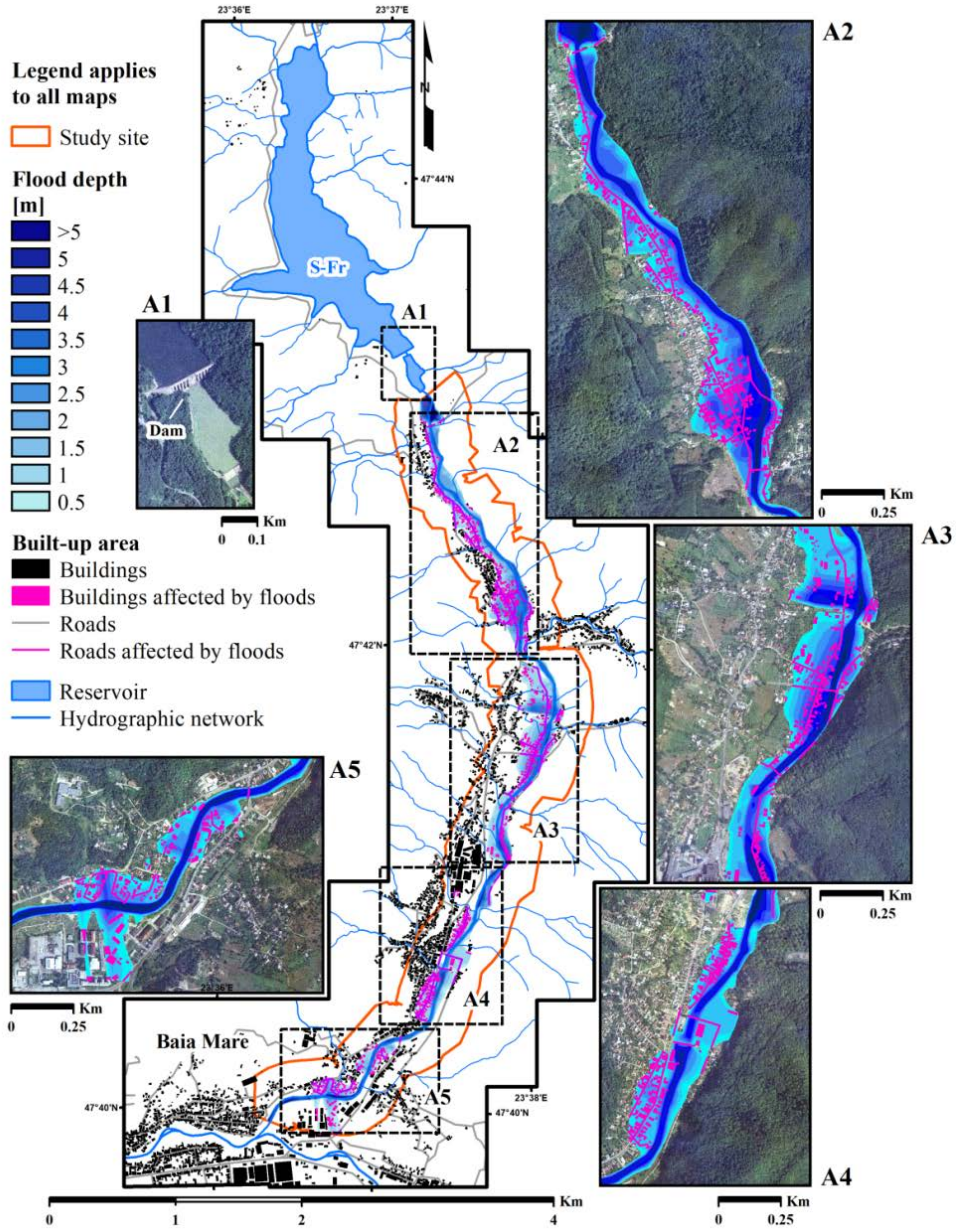

Figure 7. FD (m) within urban area located computed for each scenario with 5%, 1% and 0.1% return periods (A1-A5: zoom into the study area).

class, 12.32% in the H2 hazard class, 13.89% in the H3 hazard class, 8.79% in the H4 hazard class, 14.26% in the H5 hazard class and 16.72% in the H6 hazard class. Within the urban area 380 buildings are affected by the flood wave, of which: 234 buildings in the H1 hazard class, 59 constructions in the H2 hazard class, 59 houses in the H3 hazard class, 26 buildings in the H4 hazard class and two isolated houses in the H5 hazard class (Table 6).

4.2. Flood hazard (FH) assessment

The FH maps obtained for each scenario with 5%, 1% and 0.1% return periods (Figure 9) was generated using 2D models according to AIDR (2017). Therefore, the FD and FV rasters has been used to classify the flood impact into six hazard classes (see Table 2 and Table 6).

Based on the S1 (5% return period) a maximum value of 20.62 m^2/s was registered and the distribution of the affected areas are: 28.13% in the H1 hazard class, 13.47% in the H2 hazard class, 16.5% in the H3 hazard class, 12.09% in the H4 hazard class, 12.12% in the H5 hazard class and 17.68% in the H6 hazard class. Based on the S2 (1% return period) in the urban area 609 constructions are affected by FH according to 1% (100-year) return period, of which: 294 buildings in the H1 hazard class, 100 houses in the H2 hazard class, 124

buildings in the H3 hazard class, 56 constructions in the H4 hazard class, 34 houses in the H4 hazard class and one building in the H6 hazard class (Table 6, Figure 10).

Table 6. FH classes, surface area (ha) and number of buildings affected by flood computed for each scenario with 5%, 1% and 0.1% return periods

FH classes	S1 – 5%		S2 – 1%		S3 – 0.1%	
	Surface (ha)	No. buildings	Surface (ha)	No. buildings	Surface (ha)	No. buildings
H1	18.47	234	21.24	294	23.98	337
H2	6.69	59	10.17	100	9.77	116
H3	7.54	59	12.46	124	17.41	141
H4	4.77	26	9.13	56	17.23	202
H5	7.74	2	9.15	34	16.44	97
H6	9.08	-	13.35	1	19.26	17

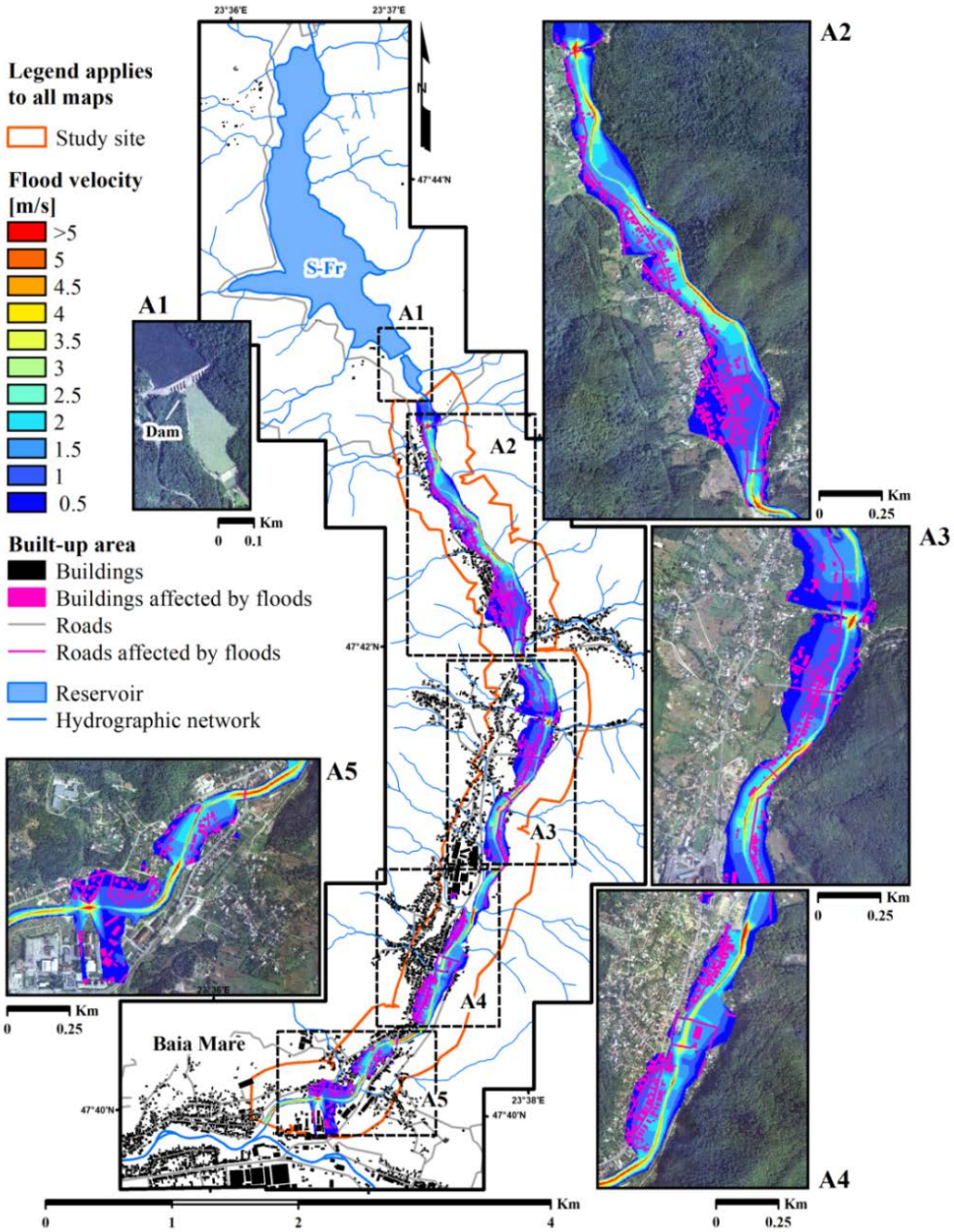

Figure 8. FV (m/s) within urban area located computed for each scenario with 5%, 1% and 0.1% return periods (A1-A5: zoom into the study area).

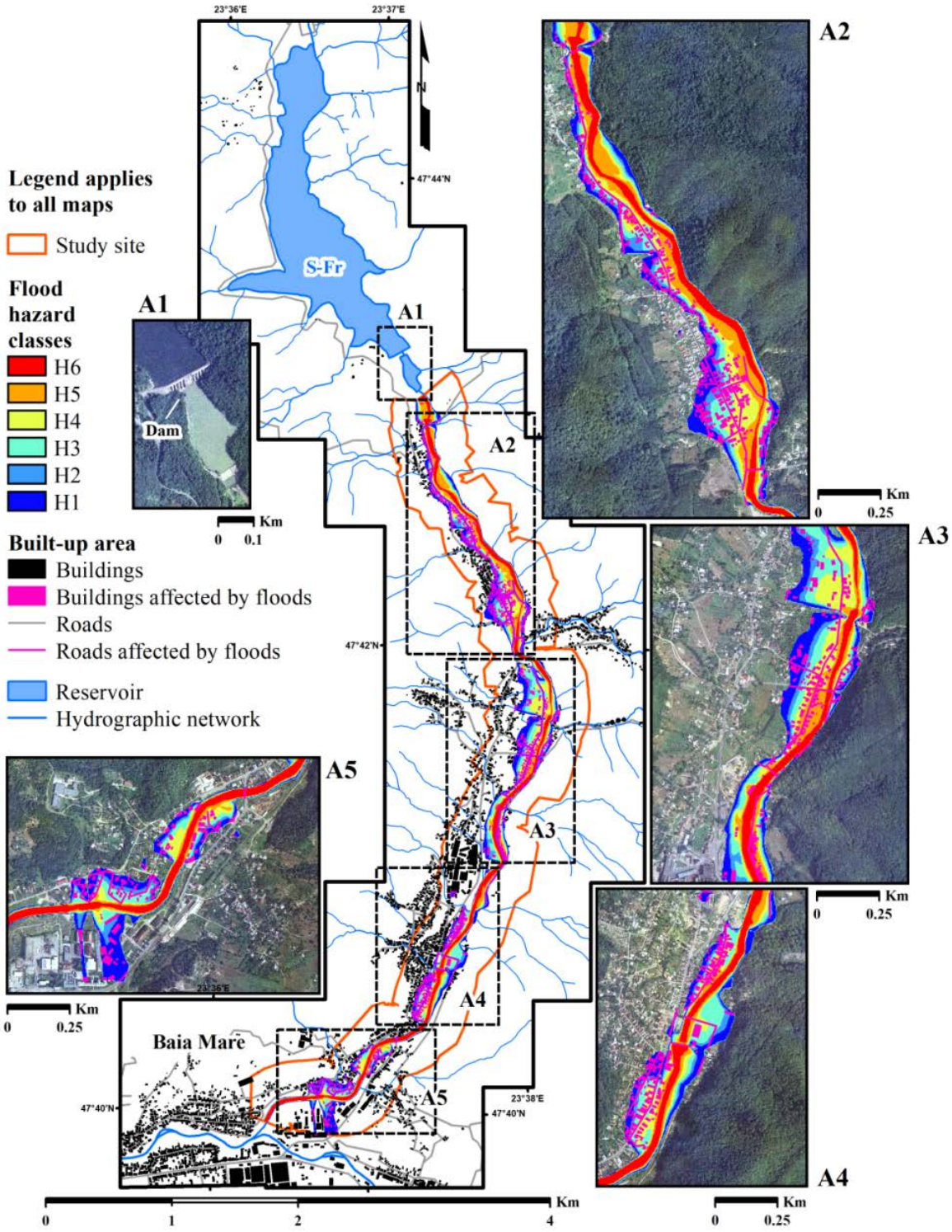

Figure 9. FH classification (see Table 3) within urban area located computed for each scenario with 5%, 1% and 0.1% return periods (A1-A5: zoom into the study area).

In the S3 (0.1% return period) the maximum value of FD·FV registered was of the 35.49 m^2/s (Figure 9). In the study site, 23.04% of the total affected area is in the H1 hazard class, 9.39% in the H2 hazard class, 16.73% in the H3 hazard class, 16.55% in the H4 hazard class, 15.79% in the H5 hazard class and 18.5% in the H6 hazard class. In this scenario, is noteworthy the high proportion of surfaces affected by H6 hazard class (18.5%) which indicates the flood wave magnitude along to the Firiza Valley. Therefore, the flood impact on the built-up area is also significant: 337 buildings in the H1 hazard class, 116 houses in the H2 hazard class, 141 constructions in the H3 hazard class, 202 buildings in the H4 hazard class, 97 houses

in the H4 hazard class and 17 constructions in the H6 hazard class (Table 6, Figure 10).

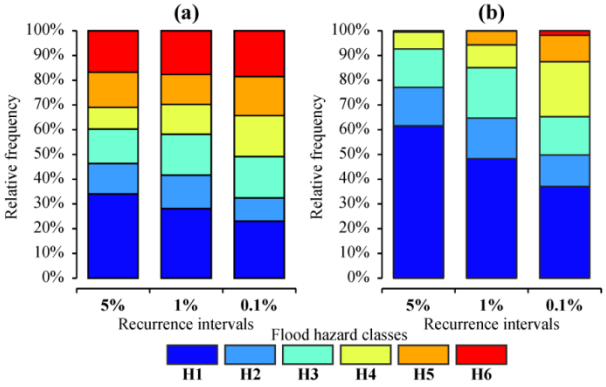

Figure 10. FH classes distribution for **(a)** potentially FE area and **(b)** potentially affected buildings based on FH classification criteria (see Table 2). HEC-RAS scenarios with 5%, 1% and 0.1% return periods in each chart.

5. DISCUSSION

Inside of highly modified water environments (e.g., regulated river sectors, floodplains equipped with dams, reservoirs and other hydro-technical works) which overlaid with urbanized areas, floods and their associated phenomena can cause a tremendous number of damages (Afzal et al., 2022; Bellos et al., 2022; Iroume et al., 2022; Romanescu et al., 2017; Tošić et al., 2022; Urzică & Grozavu, 2021). Even in well-designed river systems (e.g., lower Firiza Valley), flood disasters exist, and populated area is in danger due to a human or accidentally error in the discharge flow at the spillway gate. The best example in Romania for such an event is the historical flood event which occurred on Prut River in the period July – August 2008, downstream of the Stânca-Costești reservoir (Romanescu et al., 2011). Therefore, due to the large impact on the environment (e.g., natural, social, economic), a good preparation regarding FH assessment in the proximity of S-Fr (e.g., downstream of the dams) is always welcomed (Abdelkarim et al., 2019; Gibson et al., 2022; Mihu-Pintilie et al., 2019; Papaioannou et al., 2021; Tegos et al., 2022).

In this paper, we propose a complex methodology for FH assessment under accurate (average flow rates) and mathematical (flow rates with different return periods) hydrological data by combining LiDAR-derived DEM, 2D HEC-RAS modeling and RS techniques which complement the Action Plans for Dam Failure (APDF) and the national flood mitigation strategy. We chose this methodology because according to Sanders (2007), the LiDAR-derived DEM offer the best results within 2D flood simulations. More than that, HEC-RAS software can offer a fast solution with a low amount of data to an overview of a potential flood event being widely accepted by the scientific community and there is no license fee (Brunner, 2016a, 2016b).

In this framework, to create the 2D hydraulic model, within 4.37 km^2 floodplain extent of Firiza Valley (urban area of Baia Mare city, NW Romania), a polygonal mesh with 67,000 computational cells was created. The hydraulic detailed properties of computational cells (elevation-volume relationship) were captured using the LiDAR-derived DEM. Comparing an unsteady flow model with and steady flow model by their complexity, the unsteady flow model is more common to have instability issues (Bellos et al., 2022; Costabile et al., 2020; Dasallas et al., 2019; David & Schmalz, 2021; Üneş et al., 2020). In order to acquire a 2D hydraulic model with a high accuracy and stability we gave a huge attention to the geometric data, flow data and boundary conditions accuracy (Cedillo et al., 2021; Prior et al., 2021; Urzică & Grozavu, 2021). For the geometric data we used the grayscale 3D representation of the LiDAR derived DEM and generate the 2D flow area and the break lines. Considering the importance of the Manning's n values, we also updated the roughness coefficient based on our study area geomorphological characteristics and land-use categories. According to Brunner (2016b) there is an inversely relationship between Manning coefficient and FV (e.g., a high value of the roughness coefficient leads to a low FV). At the end of our work, we also compared the 2D HEC-RAS results with the flood maps results realized under the Directive 2007/60/EC of the EC for the flood mitigation strategy and provided by S-TWBA (Figure 11).

Overall, the comparison between 2D HEC-RAS and NARW hazard maps indicate strongs similarities along the lower Firiza Valley for all three scenarios with the exception of some densely populated areas where the NARW scenarios underestimated the FH impact. The NARW obtained a FE area of 87.45 ha, which is a difference of 16.20 ha, whereas we acquired a FE area of 103.66 ha based on 2D HEC-RAS results in the case of 0.1% return period (Figure 11a). We derived a FE area of 75.15 ha (Figure 11b) and the NARW of 15.47 ha for the 1% return period (a difference of 15.47 ha).

Figure 11c shows the FE area for the 5%, which is 54.07 ha, and the NARW area, which is 29.59 ha (a difference of 24.47 ha). The two cases with the biggest variations are 0.1% and 5%. The differences in FE area are mainly given by the spatial resolution of the DEM used for the hydrological modeling (SMIS-CSNR, 2022).

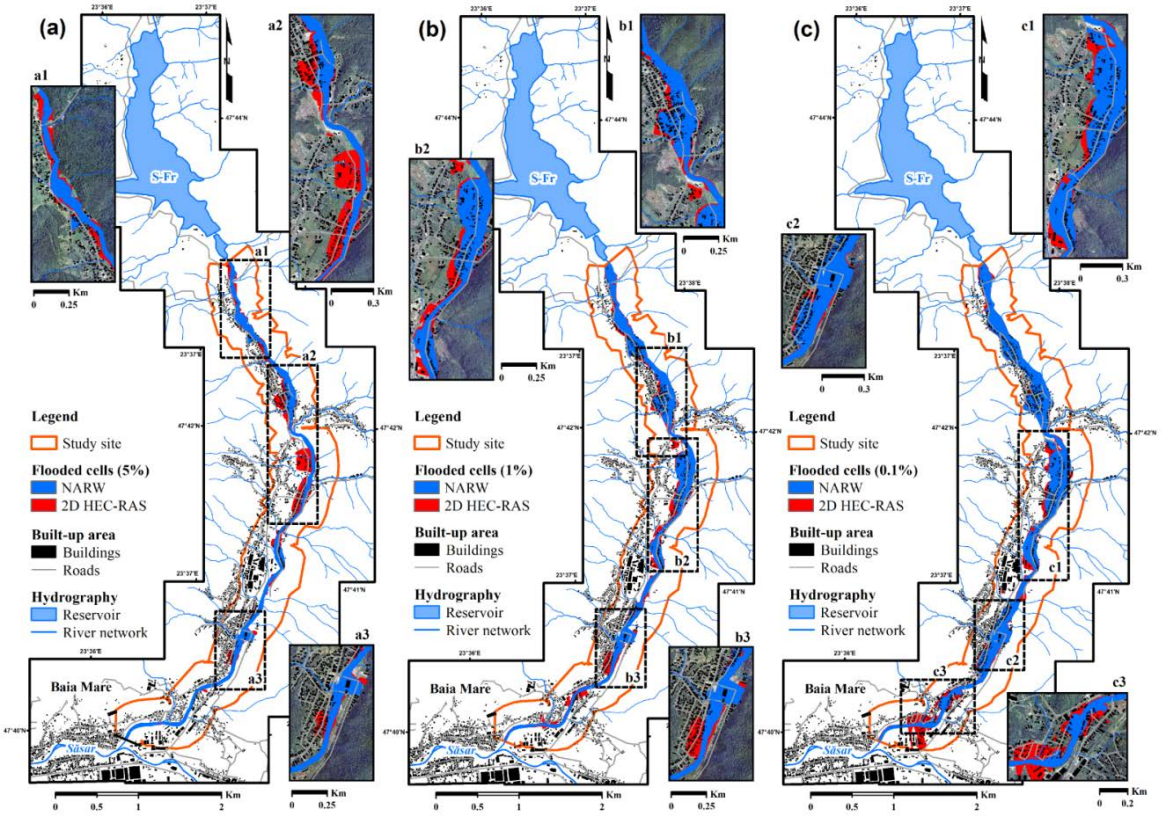

Figure 11. Comparison between official FH data (NARW) and 2D FE computed for **(a)** 5% (20-year), **(b)** 1% (100-year) and **(c)** 0.1% (1000-year) return periods.

The NARW states that risk and hazard maps for the Firiza River were created with spatial resolutions of 5 and 10 m. We used a 3 m LiDAR produced DEM with all the topographical information for our analysis (e.g., houses, attachment constructions, administrative buildings, industrial built-up area).The best results can be obtained by using DSM because this product has already integrated the solid objects of the topography. If a DSM is not available for the interest area the best option is to apply the methodology mentioned above. One more reason for the existing differences is that NARW made the hydrological modelling scenarios for the whole catchment, without taking into consideration the S-Fr while in our study we managed to create a 2D hydraulic model only for the area downstream S-Fr, thus improving the final result of hydrological modelling scenarios.

The advantages for using 2D HEC-RAS modeling is that the 2D projects are more stable than 1D projects, less time building the hydrological model, less subjective decisions (e.g., cross section, distance between cross sections), hydrodynamic animations trough RAS Mapper module. The main disadvantages about the 2D HEC-RAS are the long running time and the need of a detailed DEM (e.g., LiDAR derived DEM). The interoperability, the friendly user interface, the large community of practitioners, the RAS Mapper maps results (e.g., velocity, depth, shear stress, arrival time, duration, recession) make HEC-RAS software the best and fastest solution in flood mitigation strategy.

6. CONCLUSIONS

Integrating LiDAR data and RS-based validation techniques for 2D hydraulic modeling using HEC-RAS software produced sufficiently information to develop accurate urban FH maps downstream of S-Fr (urban area of Baia Mare City, NW Romania).

The following concluding remarks can be presented based on the FH patterns computed using various discharge releases from the S-Fr spillway gate (average discharge for evaluating the hydraulic stability of the models; calculated discharge with 5%, 1%, and 0.1% return periods): (i) The 2D multi-scenarios developed for the study site allowed to test the FCC and indicate the outflow values at S-Fr spillway gate which can cause flood events; (ii) In case of all three computed scenarios with 5%, 1% and 0.1% return periods the FE patterns within urban area of Baia Mare City indicate a potential high impact. This aspect is highlighted by the hazard maps developed using the FD and FV models obtained through the RAS Mapper module; (iii) Integrating 2D HEC-RAS modeling,

LiDAR measurements and hydrological data can be a good option to elaborate FH maps in the proximity of the big dams in order to improve the flood mitigation strategy.

Any flood mitigation strategy must include the development of flood scenarios for small to medium catchment regions since large-scale analyses (like official flood hazard maps in Romania) overestimates the impression of flood risk. Therefore, the 2D flood modeling based on LiDAR-derived DEM is essential part for every urbanized environment in the context of climate change and modern society development pressure and trends.

Acknowledgments

The authors thanks to the Romanian Waters National Administration, Someș-Tisa Water Basin Administration and Maramureș Water Management System who provided the hydrological and elevation data used in this study. Also, our thanks go to the anonymous reviewers, who helped us in improving the manuscript.

REFERENCES

Abdelkarim, A., Gaber, A.F.D., Youssef, A.M., & Pradhan, B., 2019. *Flood Hazard Assessment of the Urban Area of Tabuk City, Kingdom of Saudi Arabia by Integrating Spatial-Based Hydrologic and Hydrodynamic Modeling*. Sensors, 19, 1024. DOI: 10.3390/s19051024

Afzal, M.A., Ali, S., Nazeer, A., Khan, M.I., Waqas, M.M., Aslam, R.A., Cheema, M.J.M., Nadeem, M., Saddique, N., Muzammil, M., & Shah, A.N., 2022. *Flood Inundation Modeling by Integrating HEC–RAS and Satellite Imagery: A Case Study of the Indus River Basin*. Water, 14, 2984. DOI: 10.3390/w14192984

Ahmad, I., Wang, X., Waseem, M., Zaman, M., Aziz, F., Khan, R.Z.N., & Ashraf, M., 2022 *Flood Management, Characterization and Vulnerability Analysis Using an Integrated RS-GIS and 2D Hydrodynamic Modelling Approach: The Case of Deg Nullah, Pakistan*. Remote Sens., 14, 2138. DOI: 10.3390/rs14092138

AIDR (Australian Institute for Disaster Resilience), 2017. *Australian Disaster Resilience Handbook 7 Managing the Floodplain: A Guide to Best Practice in Flood Risk Management in Australia* (AIDR 2017). Available online: http://www.dpmc.gov.au/ government/its-honour (Accessed on 18 October 2022).

Alfieri, L., Pappenberger, F.,Wetterhall, F., Haiden, T., Richardson, D., & Salamon, P., 2014. *Evaluation of ensemble streamflow predictions in Europe*. J. Hydrol. 2014, 517, 913–922. DOI: 10.1016/j.jhydrol.2014.06.035

Albano, R., Samela, C., Crăciun, I., Manfreda, S., Adamowski, J., Sole, A., Sivertun, Å., & Ozunu, A., 2020. *Large Scale Flood Risk Mapping in Data Scarce Environments: An Application for Romania*. Water 2020, 12, 1834. DOI: 10.3390 /w12061834

Alfieri, L., Burek, P., Feyen, L., & Forzieri, G., 2015. *Global warming increases the frequency of river floods in Europe*. Hydrol. Earth Syst. Sci. 19, 2247–2260. DOI: 10.5194/hess-19-2247-2015

Arief, H.A., Strand, G.-H., Tveite, H., & Indahl, U.G., 2018. *Land Cover Segmentation of Airborne LiDAR Data Using Stochastic Atrous Network.* Remote Sens. 10(6), 973. DOI: 10.3390/rs10060973

Armenakis, C., Du, E.X., Natesan, S., Persad, R.A., & Zhang, Y., 2017. *Flood Risk Assessment in Urban Areas Based on Spatial Analytics and Social Factors*. Geosciences, 7, 123. DOI: 10.3390/geosciences7040123

Arseni, M., Rosu, A., Calmuc, M., Calmuc, V.A., Iticescu, C., & Georgescu, L.P., 2020. *Development of Flood Risk and Hazard Maps for the Lower Course of the Siret River, Romania.* Sustainability, 12, 6588. DOI: 10.3390/su12166588

Awadallah, M.O.M., Juárez, A., & Alfredsen, K., 2022. *Comparison between Topographic and Bathymetric LiDAR Terrain Models in Flood Inundation Estimations.* Remote Sens., 14, 227. DOI: 10.3390/rs14010227

Bellos, V., Kourtis, I., Raptaki, E., Handrinos, S., Kalogiros, J., Sibetheros, I.A., & Tsihrintzis, V.A., 2022. *Identifying Modelling Issues through the Use of an Open Real-World Flood Dataset.* Hydrology, 9, 194. DOI: 10.3390/ hydrology9110194

Balica, S., & Wright, N.G., 2009. *A network of knowledge on applying an indicator-based methodology for minimizing flood vulnerability*. Hydrol. Process, 23, 2983–2986. DOI: 10.1002/hyp.7424

Banholzer, S., Kossin, J., & Donner, S., 2014. *The Impact of Climate Change on Natural Disasters. In Reducing Disaster: EarlyWarning Systems for Climate Change*, Singh, A., Zommers, Z., Eds., Springer: Dordrecht, The Netherlands, pp. 21–49. DOI: 10.1007/978-94-017-8598-3_2

Blöschl, G., Hall, J., Parajka, J., Perdigão, R.A.P., Merz, B., Arheimer, B., Aronica, G.T., Bilibashi, A., Bonacci, O., Borga, M., et al., 2017. *Changing climate shifts timing of European floods*. Science, 357, 588–590. DOI: 10.1126/science.aan2506

Bubeck, P., Kreibich, H., Penning-Rowsell, E.C., Botzen, W.J.W., De Moel, H., & Klijn, F., 2017. *Explaining differences in flood management approaches in Europe and in the USA. A comparative analysis.* J. Flood Risk Manag. 10, 436–445.DOI: 10.1111/jfr3.12151

Bush, S.T., Dresback, K.M., Szpilka, C.M., & Kolar, R.L., 2022. *Use of 1D Unsteady HEC-RAS in a Coupled System for Compound Flood Modeling: North Carolina Case Study.* J. Mar. Sci. Eng. 2022, 10, 306. DOI : 10.3390/jmse10030306

Brunner, G.W., 2016a. *HEC-RAS River Analysis System, 2D Modeling User's Manual, Version 5.0.* Available online: https://www.hec.usace. army.mil (Accessed

on 01 September 2020).

Brunner, G.W., 2016b. *CEIWR-HEC. HEC-RAS River Analysis System, 2D Modeling User's Manual; Version 5.0*. Available online: https://www.hec.usace.army.mil/software/hec-ras/documentation (Accessed on 19 October 2022).

Brunner, G.W., 2020. *CEIWR-HEC. Modeler Application Guidance for steady versus Unsteady, and 1D versus 2D versus 3D Hydraulic Modeling.* Available online: https://www.hec.usace.army.mil (Accessed on 19 October 2022).

Cammerer, H., Thieken, A.H., & Verburg, P.H., 2013. *Spatio-temporal dynamics in the flood exposure due to land use changes in the Alpine Lech Valley in Tyrol (Austria).* Nat. Hazards, 68, 1243–1270. DOI: 10.1007/s110 69-012-0280-8

Cedillo, S., Sánchez-Cordero, E., Timbe, L., Samaniego, E., & Alvarado, A., 2021. *Patterns of Difference between Physical and 1-D Calibrated Effective Roughness Parameters in Mountain Rivers*. Water, 13, 3202. DOI: 10.3390/w13223202

Cîmpianu, C.I., & Mihu-Pintilie, A., 2018. *Mapping Floods Using Open Source Data and Software - Sentinel-1 and ESA Snap*. In Proceedings of the 4th International Scientific Conference Geobalcanica 2018: International Scientific Conference Geobalcanica, Ohrid, Republic of Macedonia, 4, 521-529.

Cîmpianu, C.I., Mihu-Pintilie, A., Stoleriu, C.C., Urzică, A., & Huţanu, E., 2021. *Managing Flood Hazard in a Complex Cross-Border Region Using Sentinel-1 SAR and Sentinel-2 Optical Data: A Case Study from Prut River Basin (NE Romania).* Remote Sens. 2021, 13, 4934. DOI: 10.3390/rs13234934

Ciurte, D.L., Mihu-Pintilie, A., Paveluc, L.E., & Stoleriu, C.C., 2019. *50 year's determination of reservoir sedimentation rate using topography measurements and GIS. Case study: Strîmtori-Firiza Reservoir*, Baia Mare, Romania. Geobalcanica Society Proceedings 2019, 590–596. DOI: 10.18509/GBP.2019.69

Clarke, B., Otto, F., Stuart-Smith, R., & Harrington, L., 2022. *Extreme weather impacts of climate change: an attribution perspective.* Environ. Res.: Climate, 012001. DOI: 10.1088/2752-5295/ac6e7d

Costache, R., Barbulescu, A., & Pham, Q.B., 2021. *Integrated Framework for Detecting the Areas Prone to Flooding Generated by Flash-Floods in Small River Catchments.* Water, 13, 758. DOI: 10.3390/w13060758

Costabile, P., Costanzo, C., Ferraro, D., Macchione, F., & Petaccia, G., 2020 *Performances of the New HEC-RAS Version 5 for 2-D Hydrodynamic-Based Rainfall-Runoff Simulations at Basin Scale: Comparison with a State-of-the Art Model*. Water, 12, 2326. DOI: 10.3390/w12092326

David, A., & Schmalz, B., 2021. *A Systematic Analysis of the Interaction between Rain-on-Grid-Simulations and Spatial Resolution in 2D Hydrodynamic Modeling*. Water, 13, 2346. DOI: 10.3390/w13172346

Dasallas, L., Kim, Y., & An, H., 2019. *Case Study of HEC-RAS 1D–2D Coupling Simulation: 2002 Baeksan Flood Event in Korea*. Water, 11, 2048. DOI: 10.3390/w11102048

Do, H.X., Zhao, F., Westra, S., Leonard, M., Gudmundsson, L., Boulange, J.E.S., Chang, J., Ciais, P., Gerten, D., Gosling, S.N., Müller Schmied, H., Stacke, T., Telteu, C.-E., & Wada, Y., 2020. *Historical and future changes in global flood magnitude - evidence from a model–observation investigation*. Hydrol. Earth Syst. Sci., 24, 1543–1564. DOI:10.5194/hess- 24-1543-2020

Dobrovičová, S., Dobrovič, R., & Dobrovič, J., 2015. *The Economic Impact of Floods and their Importance in Different Regions of the World with Emphasis on Europe.* Procedia Econ. Financ. 34, 649–655 DOI: 10.1016/S2212-5671(15)01681-0

Feng, B., Zhang, Y., & Bourke, R., 2021 *Urbanization impacts on flood risks based on urban growth data and coupled flood models*. Nat. Hazards, 106, 613–627. DOI: 10.1007 /s11069-020-04480-0

Feranec, J., Jaffrain, G., Soukup, T., & Hazeu, G., 2010. *Determining changes and flows in European landscapes 1990–2000 using CORINE land cover data.* Appl. Geogr. 30, 19–35. DOI: 10.1016/j.apgeog.2009.07.003

Gallegos, H.A., Schubert, J.E., & Sanders, B.F., 2009. Two-dimensional, high-resolution modeling of urban dam-break flooding: A case study of Baldwin Hills, California. Adv. Water Resour. 32, 1323–1335. DOI: 10.1016/ j.advwatres. 2009.05.008

Gibson, S., Moura, L.Z., Ackerman, C., Ortman, N., Amorim, R., Floyd, I., Eom, M., Creech, C., & Sánchez, A., 2022. *Prototype Scale Evaluation of Non-Newtonian Algorithms in HEC-RAS: Mud and Debris Flow Case Studies of Santa Barbara and Brumadinho*. Geosciences, 12, 134. DOI: 10.3390/geo sciences12030134

Gigović, L., Pamučar, D., Bajić, Z., & Drobnjak, S., 2017. *Application of GIS Interval Rough AHP Methodology for Flood Hazard Mapping in Urban Areas.* Water, 9, 360. DOI: 10.3390/ w9060360

Gralepois, M., Larrue, C., Wiering, M., Crabbé, A., Tapsell, S., Mees, H., Ek, K., & Szwed, M., 2016. *Is flood defense changing in nature? Shifts in the flood defense strategy in six European countries*. Ecol. Soc. 21(4), 37. DOI: 10.5751/ ES-08907-210437

Hall, J., Arheimer, B., Aronica, G.T., Bilibashi, A., Boháč, M., Bonacci, O., Borga, M., Burlando, P., Castellarin, A., Chirico, G.B., et al., 2015. *A European Flood Database: Facilitating comprehensive flood research beyond administrative boundaries*. Proc. Int. Assoc. Hydrol. Sci., 370, 89–95, DOI: 10. 5194/piahs-370- 89-2015

Hirabayashi, Y., Mahendran, R., Koirala, S., Konoshima, L., Yamazaki, D., Watanabe, S., Kim, H., & Kanae, S., 2013. *Global flood risk under climate change. Nature Clim. Change* 2013, 3, 816–

82. DOI: 10.1038/ncli mate1911

Hoeppe, P., 2016. *Trends in weather related disasters—Consequences for insurers and society.* Weather Clim. Extrem. 11, 70–79.DOI: 10.1016/j.wace.2015.10.002

Holguin, N., Mugica, A., & Ukar, O., 2021. *How Is Climate Change Included in the Implementation of the European Flood Directive? Analysis of the Methodological Approaches of Different Countries*. Water, 13, 1490. DOI: 10.3390/w13111490

Iroume, J.Y.-A., Onguéné, R., Djanna Koffi, F., Colmet-Daage, A., Stieglitz, T., Essoh Sone, W., Bogning, S., Olinga Olinga, J.M., Ntchantcho, R., Ntonga, J.-C., Braun, J.-J., Briquet, J.-P., & Etame, J., 2022. *The 21st August 2020 Flood in Douala (Cameroon): A Major Urban Flood Investigated with 2D HEC-RAS Modeling.* Water, 14, 1768. DOI: 10.3390/w14111768

Huang, Q., Wang, J., Li, M., Fei, M., & Dong, J., 2017. *Modeling the influence of urbanization on urban pluvial flooding: a scenario-based case study in Shanghai, China*. Nat. Hazards, 87, 1035–1055. DOI: 10.1007/s11069-017-2808-4

Dumitriu, D., 2020. *Sediment flux during flood events along the Trotuș River channel: Hydrogeomorphological approach.* J. Soils Sediments, 20, 4083–4102. DOI: 10.1007/s 11368-020-02763-4

Jonoski, A., Popescu, I., Zhe, S., Mu, Y., & He, Y., 2019. *Analysis of Flood Storage Area Operations in Huai River Using 1D and 2D River Simulation Models Coupled with Global Optimization Algorithms*. Geosciences, 9, 509. DOI: 10.3390/ geosciences9120509

Kim, Y., 2016. Generation of Land Cover Maps through the Fusion of Aerial Images and Airborne LiDAR Data in Urban Areas. Remote Sens. 8, 521. DOI: 10.3390/rs806 0521

Kucsicsa, G., Popovici, E., Bălteanu, D., Grigorescu, I., Dumitrascu, M., & Mitrica, B., 2019. *Future land use/cover changes in Romania: Regional simulations based on CLUE-S model and CORINE land cover database*. Landscape Ecol. Eng. 15, 75–90. DOI: 10.1007/s11355-018-0362-1

Kundzewicz, Z.W., Pinskwar, I., & Brakenridge, G.R., 2013. *Large floods in Europe*, 1985–2009. Hydrol. Sci. J., 58, 1–7. DOI: 10. 1080/02626667.2012.745082

Kundzewicz, Z.W., Pińskwar, I., & Brakenridge, G.R., 2018. *Changes in river flood hazard in Europe: a review*. Hydrol. Research, 49(2), 294–302. DOI: 10.2166/nh.2017.016

Lexa, J., Seghedi, I., Németh, K., Szakács, A., Konečny, V., Pécskay, Z., Fülöp, A., & Kovacs, M., 2010. *Neogene-Quaternary Volcanic forms in the Carpathian-Pannonian Region: a review*. Open Geosciences, 2(3), 207–270. DOI: 10.2478/v10085-010-0024-5

Mangini, W., Viglione, A., Hall, J., Hundecha, Y., Ceola, S., Montanari, A., Rogger, M., Salinas, J.L., Borzì, I., & Parajka, J., 2018. Detection of trends in magnitude and frequency of flood peaks across Europe. Hydrol. Sci. J., 63(4) 493-512. DOI: 10. 1080/02626667.2018.1444766

Mehedi, M.A.A., Yazdan, M.M.S., Ahad, M.T., Akatu, W., Kumar, R., & Rahman, A., 2022. *Quantifying Small-Scale Hyporheic Streamlines and Resident Time under Gravel-Sand Streambed Using a Coupled HEC-RAS and MIN3P Model*. Eng., 3, 276-300. DOI: 10.3390/eng3020021

Mitsopoulos, G., Panagiotatou, E., Sant, V., Baltas, E., Diakakis, M., Lekkas, E., & Stamou, A., 2022. *Optimizing the Performance of Coupled 1D/2D Hydrodynamic Models for Early Warning of Flash Floods*. Water, 14, 2356 DOI: 10.3390 /w14152356

Mihu-Pintilie, A., Asăndulesei, A., Nicu, I.C., Stoleriu, C.C., & Romanescu, G., 2014. *Using GPR for assessing the volume of sediments from the largest natural dam lake of the Eastern Carpathians: Cuejdel Lake, Romania*. Environ. Earth Sci. 75(8), 710. DOI: 10.1007/s12665-016-5537-1

Mihu-Pintilie, A., 2018. *Natural Dam Lakes and Their Status Within Limnological and Geographical Studies. In: Natural Dam Lake Cuejdel in the Stânişoarei Mountains, Eastern Carpathians*; Mihu-Pintilie, A. Ed.; Springer, Cham. p. 234. DOI: 10.1007/978-3-319-77213-4_2

Mihu-Pintilie, A., Cîmpianu, C.I., Stoleriu, C.C., Pérez, M.N. & Paveluc, L.E., 2019. *Using High-Density LiDAR Data and 2D Streamflow Hydraulic Modeling to Improve Urban Flood Hazard Maps: A HEC-RAS Multi-Scenario Approach.* Water, 11(9), 1832. DOI: 10.3390/w11091832

Mustafa, A., Bruwier, M., Archambeau, P., Erpicum, S., Pirotton, M., Dewals, B., & Teller, J., 2018. *Effects of spatial planning on future flood risks in urban environments.* J. Environ. Manag. 225, 193–204. DOI: 10.1016 /j.jenvman. 2018.07.090

Muthusamy, M., Rivas Casado, M., Salmoral, G., Irvine, T., & Leinster, P. A., 2019. *Remote Sensing Based Integrated Approach to Quantify the Impact of Fluvial and Pluvial Flooding in an Urban Catchment.* Remote Sens. 11, 577. DOI: 10.3390/rs11050577

Najibi, N., Devineni, N., 2018. *Recent trends in the frequency and duration of global floods*. Earth Syst. Dynam., 9, 757–783. DOI: 10.5194/esd-9-757-2018

Papaioannou, G., Vasiliades, L., Loukas, A., Alamanos, A., Efstratiadis, A., Koukouvinos, A., Tsoukalas, I., & Kossieris, P., 2021. *A Flood Inundation Modeling Approach for Urban and Rural Areas in Lake and Large-Scale River Basins*. Water, 13, 1264. DOI: 10.3390/w13091264

Popa, M.C., Peptenatu, D., Drăghici, C.C., & Diaconu, D.C., 2019 *Flood Hazard Mapping Using the Flood and Flash-Flood Potential Index in the Buzău River Catchment, Romania*. Water, 11, 2116. DOI: 10.3390/ w11102116

Pradhan, B., Hagemann, U., Tehrany, M.S., & Prechtel, N., 2014. *An easy to use ArcMap based texture analysis program for extraction of flooded areas*

from TerraSAR-X satellite image. Comput. Geosci. 63, 34–43. DOI: 10. 1016/ j.cageo.2013.10.011

Priest, S.J., Suykens, C., Van Rijswick, H.F.M.W., Schellenberger, T., Goytia, S.B., Kundzewicz, Z.W., Van Doorn-Hoekveld, W.J., Beyers, J.-C., & Homewood, S., 2016. *The European Union approach to flood risk management and improving societal resilience: Lessons from the implementation of the Floods Directive in six European countries.* Ecol. Soc. 21, 50. DOI: 10.5751 /ES-08913-210450

Prior, E.M., Aquilina, C.A., Czuba, J.A., Pingel, T.J., & Hession, W.C., 2021. *Estimating Floodplain Vegetative Roughness Using Drone-Based Laser Scanning and Structure from Motion Photogrammetry.* Remote Sens. 13, 2616. DOI: 10.3390/rs13132616

Rahman, M., Ningsheng, C., Mahmud, I.G., Islam, M.M., Pourghasemi, H.R., Ahmad, H., Habumugisha, J.M., Washakh, R.M.A., Alam, M., Liu, E., Han, Z., Ni, H., Shufeng, T., & Dewan, A., 2021. *Flooding and its relationship with land cover change, population growth, and road density*. Geosci. Front. 12(6), 101224. DOI: 10.1016/j.gsf.2021 .101224

Rahmstorf, S., & Coumou, D., 2011. *Increase of extreme events in a warming world.* PNAS, 108(44), 17905–17909. DOI: 10.1073/pnas.11 01766108

Romanescu, G., Stoleriu, C.C., & Romanescu, A.-M., 2011. *Water reservoirs and the risk of accidental flood occurrence. Case study: Stanca–Costesti reservoir and the historical floods of the Prut river in the period July–August 2008, Romania*. Hydrol. Process., 25, 2056–2070. DOI: 10.1002/hyp.7957

Romanescu, G., Cîmpianu, C.I., Mihu-Pintilie, A. & Stoleriu, C.C., 2017. *Historic flood events in NE Romania (post-1990).* Journal of Maps, 13(2), 787–798. DOI: 10.1080/17445647. 2017.1383944

Romanescu, G., Mihu-Pintilie, A., Stoleriu, C.C., Carboni, D., Paveluc, L. & Cîmpianu, C.I., 2018. *A Comparative Analysis of Exceptional Flood Events in the Context of Heavy Rains in the Summer of 2010: Siret Basin (NE Romania) Case Study*. Water, 10(2), 216. DOI: 10.20944/preprints201801.0078.v1

Romanescu, G., Stoleriu, C.C. & Mihu-Pintilie, A., 2020. *Implementation of EU Water Framework Directive (2000/60/EC) in Romania—European Qualitative Requirements.* In *Water Resources Management in Romania*, Negm, A., Romanescu, G., Zeleňáková, M. Eds., Springer Water. Springer, Cham: Switzerland, pp. 17-55. DOI: 10.1007/978-3-030-22320-5_2

RGIES (Romanian General Inspectorate for Emergency Situations). Ordinance 1422/192 from 16 May 2012 on the regu-lation of emergencies generated by floods, dangerous meteorological phenomena, accidents at hydrotechnical con-structions, accidental pollution on watercourses and marine pollution in the coastal area. Available online: http://legislatie.just.ro/Public/DetaliiDocument/141181 (Accessed on 14 October 2022).

Rusu, A., Ursu, A., Stoleriu, C.C., Groza, O., Niacșu, L., Sfîcă, L., Minea, I., & Stoleriu, O.M., 2020. *Structural Changes in the Romanian Economy Reflected through Corine Land Cover Datasets.* Remote Sens. 12, 1323. DOI: 10.3390/rs12081323

RWNA. (Romanian Waters National Administration). Hazard and risk flood maps. Available online: http://gis2.rowater .ro:8989/flood/ (Accessed on 14 October 2022).

Sabău, D., Șerban, G., Tudose, T., & Petrea, D., 2022. *Correlation between precipitation and orography - key element of the Spatial Decision Support System for Prevention and Management of Floods in the Firiza Basin (Northwest Romanian Carpathians).* Forum geografic, XXI(1), 5–17. DOI: 10.5775/fg. 2022.045.i

Sanders, B.F., 2007. *Evaluation of on-line DEMs for flood inundation modeling.* Adv. Water Res. 30, 1831–1843. DOI: 10.1016/j.adv watres.2007.02.005

Samanta, S., Pal, D.K., & Palsamanta, B., 2018. *Flood susceptibility analysis through remote sensing, GIS and frequency ratio model*. Appl. Water. Sci., 8, 66. DOI: 10.1007/s13201-018-0710-1

Samarasinghe, J.T., Basnayaka, V., Gunathilake, M.B., Azamathulla, H.M., & Rathnayake, U., 2022. *Comparing Combined 1D/2D and 2D Hydraulic Simulations Using High-Resolution Topographic Data: Examples from Sri Lanka—Lower Kelani River Basin*. Hydrology, 9, 39. DOI: 10.3390/hydrology 9020039

Serinaldi, F., Loecker, F., & Kilsby, C.G., 2018. *Flood propagation and duration in large river basins: a data-driven analysis for reinsurance purposes.* Nat. Hazards, 94, 71–92. DOI: 10.1007/s11069-018-3374-0

Schneider, C., Laize, C.L.R., Acreman, M.C., & Flörke, M., 2013. *How will climate change modify river flow regimes in Europe?* Hydrol. Earth Syst. Sci., 17, 325–339. DOI: 10.5194 /hess-17-325-2013

Stoleriu, C.C., Urzică, A. & Mihu-Pintilie, A., 2020. *Improving flood risk map accuracy using high-density LiDAR data and the HEC-RAS river analysis system: A case study from north-eastern Romania*. Journal of Flood Risk Management, 13 (Suppl. 1), e12572. DOI: 10. 1111/jfr3.12572

SMIS-CSNR 28988 (Someș-Tisa Water Basin Administration) The plan for the prevention, protection and mitigation of the effects of floods in the Someș-Tisa River Basin. Available online: http://www.romair.ro (Accessed on 14 October 2022).

Şerban, G., Sabău, D., Bătinaș, R., Brețcan, P., Ignat, E., & Nacu, S., 2020. *Water Resources from Romanian Upper Tisa Basin In Water Resources Management in Romania*, Negm, A., Romanescu, G., Zeleňáková, M. Eds., Springer Water. Springer, Cham: Switzerland, pp. 393–434. DOI: 10.1007/978-3-030-22320-5_2

Tabari, H., 2020. *Climate change impact on flood and extreme precipitation increases with water*

availability. Sci. Rep. 10, 13768. DOI: 10.1038/s41598-020-70816-2

Tegos, A., Ziogas, A., Bellos, V., & Tzimas, A., 2022. *Forensic Hydrology: A Complete Reconstruction of an Extreme Flood Event in Data-Scarce Area.* Hydrology, 9, 93. DOI: 10. 3390/hydrology9050093

Teng, J., Jakeman, A.J., Vaze, J., Croke, B.F.W., Dutta, D., & Kim, S., 2017. *Flood inundation modelling: A review of methods, recent advances and uncertainty analysis.* Environ. Model. Softw. 90, 201–216. DOI: 10.1016/j. envsoft.2017.01.006

Thober, S., Kumar, R., Wanders, N., Marx, A., Pan, M., Rakovec, O., Samaniego, L., Sheffield, J., Wood, E.F., & Zink, M., 2018. *Multi-model ensemble projections of European river floods and high flows at 1.5, 2, and 3 degrees global warming*. Environ. Res. Lett. 2018, 13, 014003. DOI: 10.1088 /1748-9326/aa9e35

Tošić, R., Blagojević, V., Trifković, M., Sudar, T., Dragićević, S., Lovrić, N., & Topalović, Ž., 2022: *A methodology for mapping areas under torrential flood risk: case study - the Rebrovački Brook Basin/Banja Luka municipality (B&H)*. Carpathian Journal of Earth and Environmental Sciences, 17(2), 307–322. DOI: 10.26471/cjees/2022/017/224

Üneş, F., Ziya Kaya, Y., Varçin, H., Demirci, M., Taşar, B., & Zelenakova, M., 2020. *Flood Hydraulic Analyses: A Case Study of Amik Plain, Turkey*. Water, 12, 2070. DOI: 10.3390 /w12072070

Urzică, A., Mihu-Pintilie, A., Stoleriu, C.C., Cîmpianu, C.I., Huţanu, E., Pricop, C.I., & Grozavu, A., 2021. *Using 2D HEC-RAS Modeling and Embankment Dam Break Scenario for Assessing the Flood Control Capacity of a Multi-Reservoir System (NE Romania).* Water, 13, 57. DOI: 10.3390/w130 10057

Urzică, A., & Grozavu A., 2021. *Flood hazard assessment in the joint floodplain sector of Başeu and Prut rivers (NE Romania) by reconstructing historical flood events*. Carpathian Journal of Earth and Environmental Sciences, 16(2), 275–286. DOI:10.26471/cjees/2021/016/173

Vojtek, M., & Vojteková, J., 2016. *Flood hazard and flood risk assessment at the local spatial scale: A case study.* Geomat. Nat. Haz. Risk, 7, 1973–1992. DOI: 10.1080/19475705.2016. 1166874

Quiroga, V.M., Kure, S., Udo, K., & Mano, A., 2016. *Application of 2D numerical simulation for the analysis of the February 2014 Bolivian Amazonia flood: Application of the new HEC-RAS version 5*. Ribagua, 3, 25–33. DOI: 10. 1016/j.riba.2015.12.001

Wallemacq, P., Guha-Sapir, D., & McClean, D., 2015. *CRED, UNISDR. The Human Cost of Weather Related Disasters: 1995–2015*, Centre for Research on the Epidemiology of Disasters, UNISDR: Louvain, Belgium, p. 30. Available online: https://www.unisdr.org (accessed on 02 October 2022).

Wan, W., Liu, B., Zeng, Z., Chen, X., Wu, G., Xu, L., Chen, X., & Hong, Y., 2019. *Using CYGNSS Data to Monitor China's Flood Inundation during Typhoon and Extreme Precipitation Events in 2017*. Remote Sens., 11, 854. DOI: 10.3390/ rs11070854

Wheater, H., & Evans, E., 2009. *Land use, water management and future flood risk.* Land Use Policy, 26, S251–S264. DOI: 10.1016/j.land usepol.2009.08.019

Wilby, R.L., & Keenan, R., 2012. *Adapting to flood risk under climate change*. Prog. Phys. Geogr. Earth Environ. 36, 348–378. DOI: 10.1177 /0309133312438908

Yazdan, M.M.S., Ahad, M.T., Kumar, R., & Mehedi, M.A.A., 2022. *Estimating Flooding at River Spree Floodplain Using HEC-RAS Simulation.* J Multidisciplinary Sci. J., 5, 410-426. DOI : 10.3390/j5040028

Yu, B., Liu, H., Wu, J., Hu, Y., & Zhang, L., 2010. *Automated derivation of urban building density information using airborne LiDAR data and object-based method*. Landscape Urban Plan. 98(3-4), 210-219, DOI: 10.1016 /j.l andurbplan.2010.08.004

Received at: 22. 11. 2022
Revised at: 28. 01. 2023
Accepted for publication at: 01. 02. 2023
Published online at: 03. 02. 2023